

## Article

# Elucidation of Microstructural and Mechanical Properties of Coconut Husk Mortar as a Sustainable Building Material for Ferrocement

Kalaivani Kumarasamy, Gunasekaran Kandasamy \*  and Annadurai Ramasamy

Department of Civil Engineering, SRM Institute of Science and Technology, Kattankulathur, Chennai 603203, India

\* Correspondence: gunasekk@srmist.edu.in; Tel.: +91-9443353507

**Abstract:** The main objective of this study is to use coconut husk to produce mortar for ferrocement. Mortar mix proportions are selected per ACI codes' recommendation and the WRD Handbook. Four types of mortars: Cement and River Sand mortar (CSM), Cement, River Sand and Steel fibre mortar (CSSFM), Cement and Coconut Husk mortar (CCHM), and Cement, River Sand (60%), Coconut Husk (40%), and Steel fibre mortar (CSCHSFM) are used for this study. Microstructural studies like SEM, EDX, XRD, and FTIR analysis on cement mortar constituents and mortar mixes are studied and reported. At 3, 7, and 28 days tests of hardened mortar, such as compressive, split tensile, flexural strength, and impact strength resistance, were studied. Test results revealed that the coconut husk is innovative and sustainable and could be an alternative fine aggregate that can be utilized in place of river sand, which in turn can be used for mortar production. Since it has a lesser density which proves to be an advantage for developing lightweight mortar, it can be used for ferrocement applications.

**Keywords:** coconut husk; waste utilization; mortar; microstructural properties; hardened properties; sustainable building material



**Citation:** Kumarasamy, K.; Kandasamy, G.; Ramasamy, A. Elucidation of Microstructural and Mechanical Properties of Coconut Husk Mortar as a Sustainable Building Material for Ferrocement. *Sustainability* **2023**, *15*, 3995. <https://doi.org/10.3390/su15053995>

Academic Editor: Syed Minhaj Saleem Kazmi

Received: 15 January 2023

Revised: 14 February 2023

Accepted: 19 February 2023

Published: 22 February 2023



**Copyright:** © 2023 by the authors. Licensee MDPI, Basel, Switzerland. This article is an open access article distributed under the terms and conditions of the Creative Commons Attribution (CC BY) license (<https://creativecommons.org/licenses/by/4.0/>).

## 1. Introduction

There has been a recent trend of using alternative materials to replace river sand to make cement mortar in ferrocement applications. Cementitious composites are considered as construction materials that possess the ability to address the mounting need for high-performance, cost-effective, eco-friendly, and complex structures. The development of coconut husk mortar, which is a preferred sustainable building material, is of paramount importance. Therefore, to join hands with the "Sustainable Development Goals" (SDG) and to contribute to developing sustainable building materials, this study aims to eliminate the coconut husk waste generated from agricultural domains to develop coconut husk mortar as an innovative and sustainable building material for ferrocement. It can be stated that sustainable development brings out stability in the requirements of the environment.

The rapid expansion of the construction industry has shown a steady increase in the use of sand from rivers for different purposes, which has led to the over-exploitation of riverbeds and disrupted ecologies. To meet the demand for construction, the reclamation of river sand has increased enormously in recent decades. Excessive extraction of sand from the rivers for its utilization as fine aggregate in construction fields is responsible for river damage. Many problems have arisen, including increasing river depth, lowering of water levels, rising sea levels, and the destroying of riverbanks [1–4]. In addition, from 2010 to 2020, floods brought on changes in river flow, and their effects on biodiversity will be the biggest danger to river sand reclamation. River sand utilization in the Indian construction sector has improved from 630 to 1400 million tonnes. Due to these complications, along with the mining of river sand, many countries have banned river sand as a fine aggregate in construction fields. In addition, many countries adhere to strict river restoration regulations. While the purchase of river sand has become difficult for the construction sector, there

occurs a need for alternative solutions to be found to reduce the usage of river sand and to ignite the demand for fine aggregate in the construction sector [5–9].

In the construction field, mortar is one of the most used materials. Timely execution of mortar is crucial for construction efficiency and cost control. Intensive research has recently shown that modifying mortar attained by assimilating waste materials can improve sustainable products [10]. These efforts not only consent to economic and ecological construction but also guard against the huge usage of natural fine aggregate. Therefore, it is necessary to use any new material other than conventional materials so as not to disturb pozzolanic materials and the physical performance of cement and concrete. Improvements in the microstructures of concrete occur by filler effects in addition to the pozzolanic reaction [11,12].

Ferrocement structures are a more suitable alternative for concrete structures due to their flexible metal reinforcing materials and the spread over cement-sand mortar to cover the reinforcing material. Various methods of ferrocement structure production have been known for many years. Such structures have found application not only as cabinets for use as commercial buildings and houses but as hulls for boats and ships [13–15]. Recently, in the construction industry, ferrocement has been frequently used in both developed and developing countries, which utilizes a lot of natural resources such as river sand. Fine aggregate occupies nearly 70–80% of cement-sand mortar volume [16,17]. Thus, the appropriate utilization of fine aggregates in ferrocement as an alternative material becomes necessary for replacing river sand. Thus, using surplus from agriculture arose as an effective substitute in its own right. To date, no detailed assessment has been done on this material that exhibits its possibilities for ferrocement applications [18–20].

If the alternative materials are also from sustainable sources, it is advantageous to construction and maintenance sectors. Many researchers have investigated the performance of industrial by-products such as palm oil clinker, bottom ash, corncob ash, steel slag, copper slag, and fine rubber crumb as a fine aggregate in concrete. Some recycled aggregates that perform similar to fine aggregates are recycled glass, recycled brick, recycled concrete, recycled rubber, recycled plastic, and recycled ceramic [21–23]. Many new materials have been proposed to replace river sand, which includes quarry dust, manufacturing sand, marble dust, granite dust, crushed sand, and sandstone, all of which are non-sustainable sources. However, as result of their huge availability, many works have been attempted to investigate their suitability as a fine aggregate for concrete structures [24–28]. On the other hand, coconut shell has been utilized as a sustainable alternative coarse aggregate in concrete. A reinforced slab using coconut shell concrete has been made and is under service. Even after a decade, coconut shell concrete slabs continue their service without damage [29,30]. This practical example further assures that coconut shells can be used as a coarse aggregate in preference to conventional aggregate. However, when coconut shells are crushed, a considerable amount of coconut husk is obtained as a by-product. Coconut husk can be used as an alternative for fine aggregates since its particle size distribution is similar to conventional fine aggregates [31–33]. Interestingly, using agricultural waste products as a substitute for river sand in both concrete and ferrocement as a fine aggregate is approaching a sustainable joint resolution concerning the difficulties related to the over-extraction of river sand and soil pollution [34].

Cement mortar is a heterogeneous material. Even though it has a combination of cement and fine aggregate on a macroscopic level, the cement itself may contain non-hydrated components and a few amorphous hydration products such as ettringite needles, calcium hydroxide (CH) crystal, fibrous crystals of calcium silicate hydrates (C-S-H), and pore factors that affect the strength and durability of cement mortar. Thus, it is necessary to check whether using any new material other than conventional mortar affects pozzolanic materials and the physical performance of cement and mortar. Improvements in the microstructures of mortar occurs not only by pozzolanic reaction but also by filler effects. Since the combination of coconut husk in mortar is a novelty for ferrocement, in this investigation, coconut husk was utilized as a fine aggregate to develop a cement mortar

that can be used to develop ferrocement structures. The physical properties and mechanical strength of cement mortar were also studied. The composition of pore structure and microstructure are described using Scanning Electron Microscopy (SEM), Energy Dispersive X-ray Analysis (EDX), X-ray Diffraction Analysis (XRD), and Fourier Transform Infrared Spectroscopy (FTIR), respectively.

## 2. Materials

Ordinary Portland Cement (OPC) of grade 53 and specific gravity 3.11 was used in accordance with IS 12269:2013 [35]. Because the codes advise using a 2.36 mm maximum fine aggregate for mortar developed for ferrocement [36–39], the same size was used in this work. For conventional cement mortar, river sand of zone II as per IS 383:2016 [36] was utilized as the fine aggregate. Crushed coconut husk particle size was also evaluated using sieve analysis and was found to correspond to IS 383:2016 grading zone III [36]. The fine aggregates' specific gravity, bulk density, water absorption, and fineness modulus are listed in Table 1. Figure 1a,b show the raw coconut shells and collected coconut husk after crushing. Figure 2 depicts the relationship between particle sizes and the river sand and coconut husk that passed in a sieve analysis.

**Table 1.** Properties of aggregates used.

Properties	River Sand	Coconut Husk
Specific gravity	2.55	1.14
Bulk density	1665 kg/m <sup>3</sup>	575 kg/m <sup>3</sup>
Water absorption	–	30%
Fineness modulus	2.98	2.53



**Figure 1.** (a) Raw coconut shells and (b) coconut husk.

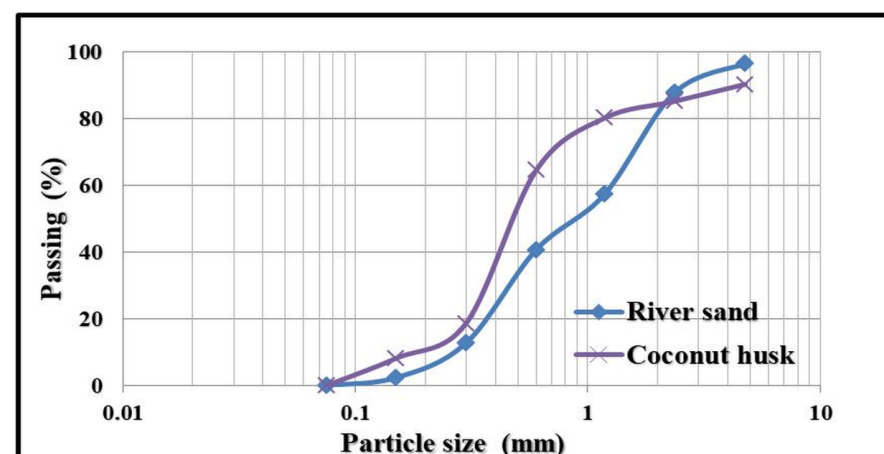


**Figure 2.** Particle size distribution of river sand and coconut husk.

### 3. Mortar Mix Proportions

Initially, the mix proportioning recommended in the ACI codes [37,38] and the WRD Handbook [39] were used as guides. For the most typical applications of ferrocement, it was proposed that the weight of the sand-to-cement ratio is 1.5 to 2.5 [37] and 1:1.5 to 1:4 [39], and the water-to-cement ratio is 0.35 to 0.50. Mortars with Cement and River Sand mortar (CSM), Cement, River Sand and Steel fibre mortar (CSSFM), Cement and Coconut Husk mortar (CCHM), and Cement, River Sand (60%), Coconut Husk (40%), and Steel fibre mortar (CSCHSFM) are utilized. The mixes of CSSFM and CSCHSFM are enhanced by incorporating crimped steel fibre at a percentage of 6, with an aspect ratio of 26. The conventional mortar with river sand achieved a minimum strength of 35 N/mm<sup>2</sup>. Based on the reference of ACI codes and the WRD handbook [37–39], the mix proportions of 1:3 (by volume) for all CSM, CSSFM, CCHM, and CSCHSFM mortar mixes were used in this investigation, despite differences in the characteristics of the materials. However, since the coconut husk has a lower density than the river sand, more volume was necessary to retain the same cement content (1:3 by volume base). Hence, the water–cement ratio obtained is 0.60, and the CCHM mix could not attain the target strength of 35 N/mm<sup>2</sup>. As a result, in the CSCHSFM mix, the coconut husk is replaced by 40% and river sand by 60%, with the same cement content of 1:3 by volume base, with a water–cement ratio of 0.40. Therefore, 1.5% superplasticizer and 6% crimped steel fibre were added to achieve the target strength of the cement mortar as suggested in the ACI Codes [37,38] and the WRD Handbook [39]. Table 2 shows a mix proportion (1:3 by volume) of different mixes and the corresponding percentage composition of constituents used.

**Table 2.** Mix proportions and percentage composition of constituents.

Mix Proportion (1:3 by Volume)	Cement (%)	Sand (%)	Coconut Husk (%)	w/c Ratio	Steel Fibre (%)	Super Plasticizer (%)
CSM	100	100	00	0.50	00	00
CSSFM		100	00	0.50	06%	00
CCHM		00	100	0.60	00	00
CSCHSFM		60	40	0.40	06%	1.5

### 4. Microstructural Studies

SEM, EDX, XRD, and FTIR were used for investigating the microstructural properties of OPC, river sand, and the coconut husk's chemical elements. Peak positions and intensities related to the patterns were examined for quantitative analysis. Table 3 shows the chemical compositions and amount of OPC in relation to the peak positions and intensities related to the EDX pattern. The FTIR is used to determine the bonding nature of materials by detecting Infrared (IR) absorptions for emissions of a liquid or solid sample in the wavelength range from 400 cm<sup>-1</sup> to 4000 cm<sup>-1</sup> [40–42]., For the CSM, CSSFM, CCHM, and CSCHSFM mortar mixes, SEM, EDX, and XRD were performed.

**Table 3.** Chemical composition of OPC, river sand, and coconut husk.

Chemical Composition (%)	OPC	River Sand	Coconut Husk
Calcium (Ca)	50.56	0.97	0.21
Oxygen (O)	30.52	45.07	48.30
Silica (Si)	8.47	33.67	0.47
Carbon (C)	7.80	8.93	49.93
Iron (Fe)	–	6.35	–
Aluminium (Al)	–	3.17	1.09
Sulphur (S)	1.39	–	–

**Table 3.** *Cont.*

Chemical Composition (%)	OPC	River Sand	Coconut Husk
Magnesium (Mg)	–	0.89	–
Potassium (K)	1.33	–	–
Sodium (Na)	–	0.56	–
Others	1.15	0.38	–

This study aimed to investigate the microstructural qualities of cement and mortar, as well as the hydration mechanisms responsible for the internal microstructures. Because the hydration process begins with the addition of water to the cement, it needs to keep track of the hydration and, as a result, the microstructures. Therefore, 0, 1, 3, 7, and 28 days were selected as the ages of the observation days on the CSM, CSSFM, CCHM, and CSCHSFM mortar mixes to verify the development of key long and thin ettringite, aggregation of fibrous crystals and clusters, and a reticular system of C-S-H.

## 5. Experimental Programme

Microstructural studies such as SEM, EDX, XRD, and FTIR analysis on cement mortar constituents and mortar mixes were selected and reported. To study the workability of cement mortar mixtures, slump and flow table tests were performed. At 3, 7, and 28 days, compressive, split tensile, and flexural strengths, and impact resistance was undertaken for hardened mortar. For slump and flow table tests, the approach indicated by IS 5512:2004 [43], ASTM C 1437-20 [44], and ASTM C 143-10 [45] was followed. Compressive strength was measured on  $150 \times 150 \times 150$  mm mortar cube specimens according to the WRD Handbook [39] and ASTM C 109 [46]. Splitting tensile strength tests were performed on cylindrical specimens using the procedure described in the WRD handbook [39] and ASTM C 496-11 [47], with cylinders gauging 150 mm in diameter and at a length of 300 mm. A flexural strength test using a simple beam of  $600 \times 50 \times 100$  mm with a mid-three-point loading, as defined in the WRD handbook [39] and ASTM C 348 [48], was conducted.

The impact resistance of the mortar mixes utilized was tested using a cylindrical disc specimen, as recommended by ACI 544.2R-89 [49]. The cylinder disc specimen utilized in this test is 152 mm in diameter and 63.5 mm thick. Concerning the hammer's mass (4.44 kg) and the fall height (457 mm), one stroke impact energy is computed to be 19.89 joules.

## 6. Results and Discussion

This section discusses the results of various tests, including microstructural properties, cement mortar consistency, and strength under compression, flexure, split tensile and impact resistance.

### 6.1. Microstructural Studies on Cement Mortar Constituents

The sample preparation of microstructural studies is furnished for the benefit of the readers. Core samples of mortar square prisms of almost  $10 \text{ mm}^2$  cut from samples using a mortar cutting machine are used for SEM and EDX analysis at the end of each curing days. Initially, the sample was flooded with acetone to stop the hydration process before it was subjected to gold sputtering to make it conductive. Electron beams from the SEM interact with the sample and produce images that can be used to determine chemical composition and phase distribution. X-ray diffraction is a technique for identifying the mineral compositions of samples or the determination of chemical assembly from crystalline materials and for identifying phases. The principle in XRD is the production of spectra that contains numerous components of various wavelengths. The definite wavelengths are the feature of the target material (generally, copper Cu). Then, the X-rays are collimated and focused. To be precise, directing X-ray beams on the sample and the diffracted X-rays are documented as a characteristic of the crystalline phases of the sample. The intensity peaks are recorded as the sample and detector are rotated. A detector records and processes an

X-ray signal and converts it to a count rate outputted to a printer device or a computer monitor. The geometry of an X-ray diffractometer is such that the rotation of the sample occurs at an angle of  $\theta$  in the path of the collimated X-ray beam. The X-ray detector rotates at an angle of  $2\theta$  and is mounted on the arm to collect the diffracted X-rays. By comparing the peaks with standards available to identify phases, the results are interpreted. For this analysis, mortar samples were ground to a fine powder of less than  $63\ \mu\text{m}$ . X-mineralogical analysis was carried out using PANalytical X'—X'per PRO with source CuK radiation (2.2 kW maximum).

As per the SEM images in Figure 3a (OPC), Figure 3b (river sand), and Figure 3c,d (coconut husk), in general, the black spots are considered pores present in the respective materials. When comparing coconut husk aggregate to river sand, it can be noticed that some pores are present, which causes an increase in the water absorption capacity of the coconut husk when compared with river sand.

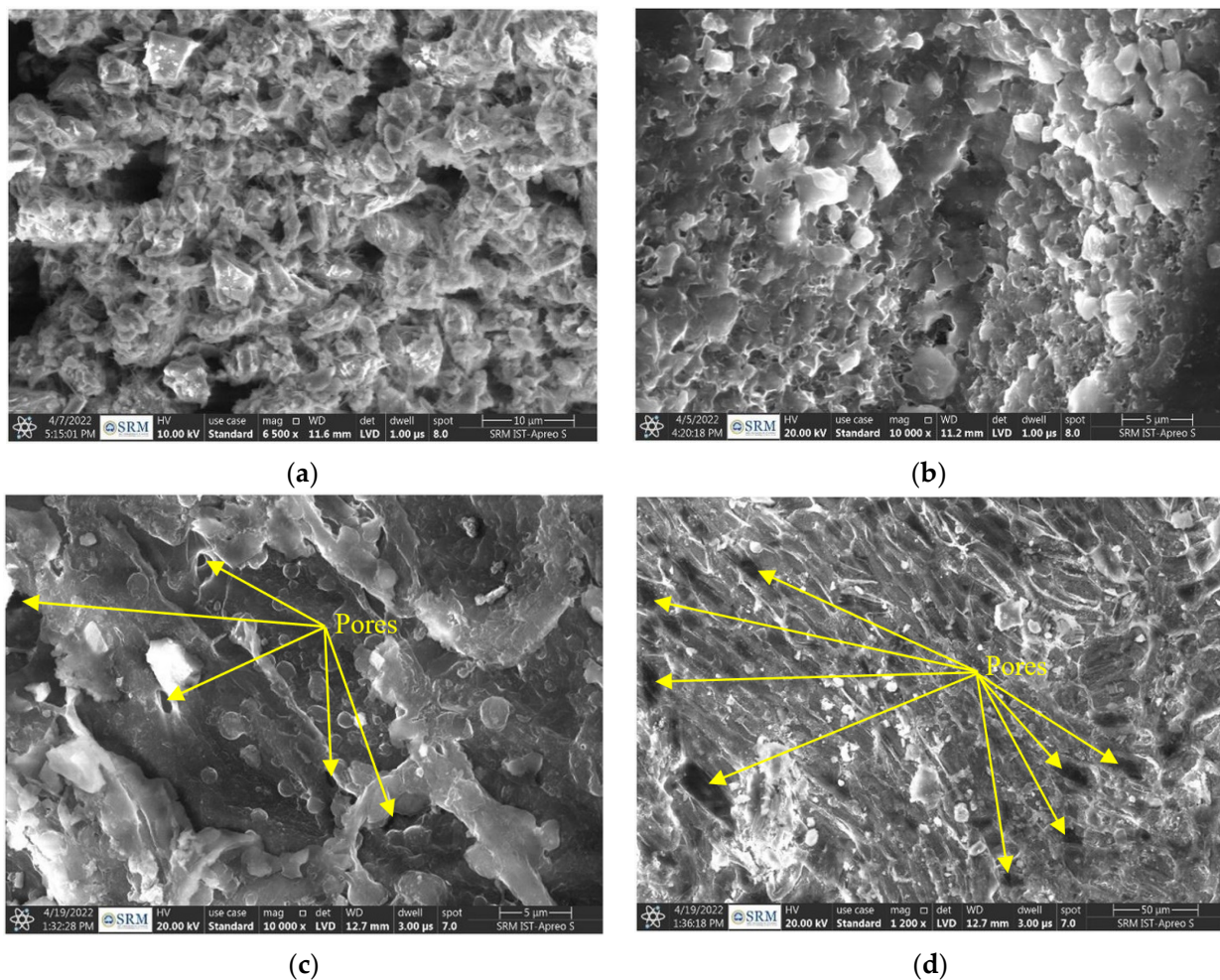


**Figure 3.** Internal microstructural image of (a) OPC, (b) river sand, and (c,d) coconut husk.

The EDX analysis of OPC, river sand, and coconut husk is shown in Figures 4–6. River sand and coconut husk are passive materials in general, and their chemical components are generally inactive, except in rare situations; thus, this study is not concentrated on the influence of chemical components in river sand and coconut husk on the production of mortar. Coconut husk is composed of cellulose, semi-cellulose, and lignin molecules in general. Carbon, hydrogen, and oxygen particles make up the molecules of cellulose, semi-cellulose, and lignin. Apart from hydrogen, helium, and lithium, EDX can identify all the stable elements.

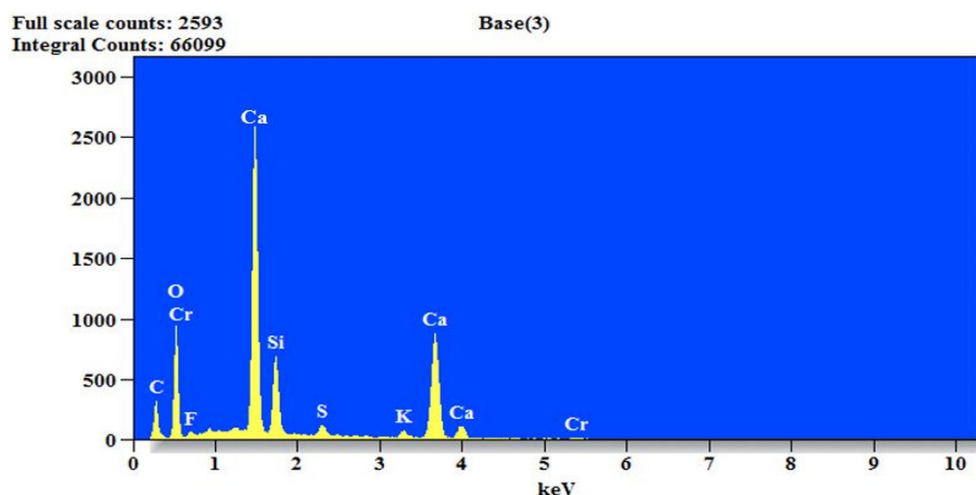


Figure 4. EDX analysis of OPC.

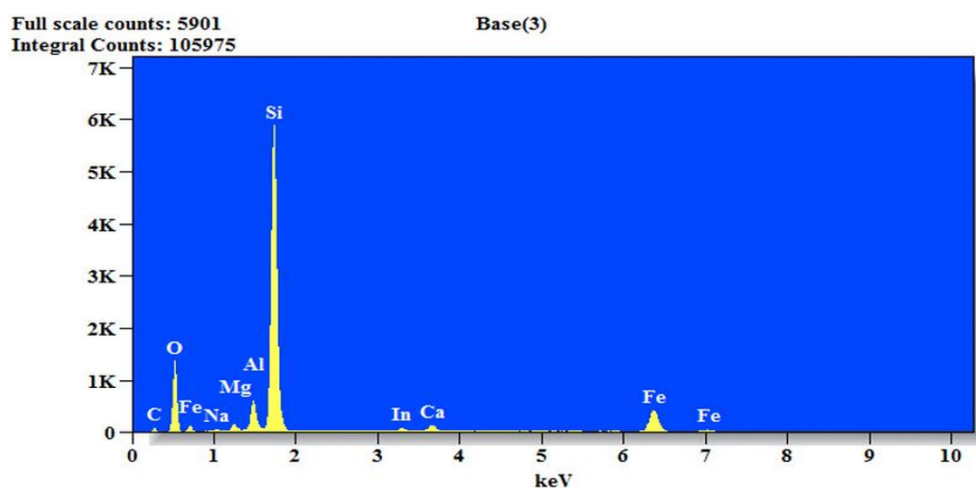


Figure 5. EDX analysis of river sand.

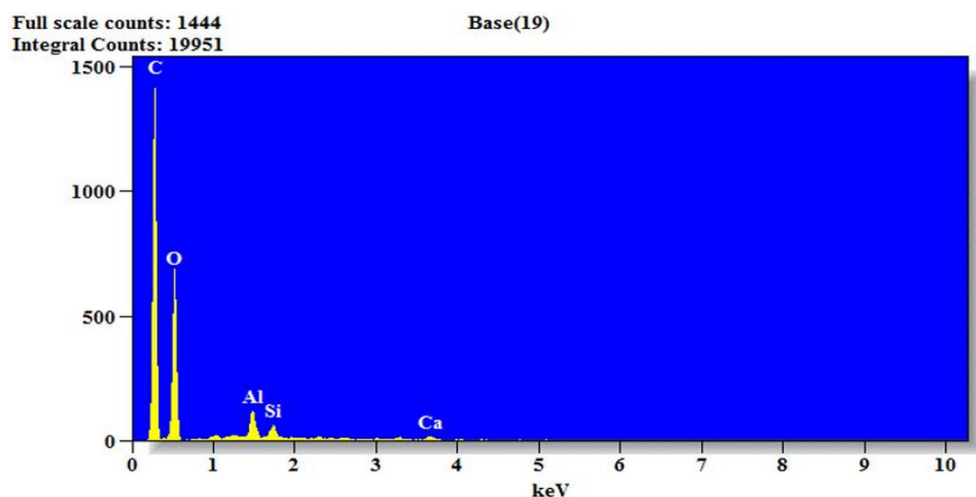


Figure 6. EDX analysis of coconut husk.

The XRD analyses crystalline powdered specimens by exposing them to X-ray beams of suitable energy. A  $2\theta$  angle ranging from  $10^\circ$  to  $90^\circ$  was used for OPC, river sand, and coconut husk, as shown in Figures 7–9. Patterns of pure phases of Bogue components were evaluated in OPC; in river sand, high silica and alumina patterns were observed, and the coconut husk was found to have a high amount of carbon [50]. An FTIR analysis of

OPC, river sand, and coconut husk are shown in Figures 10–12, respectively. In place of a molecular fingerprint of the substances examined, the FTIR signal is given as a band extending from 4000 to 400  $\text{cm}^{-1}$ . As each molecule structure produces a sole spectral fingerprint, FTIR analysis is an exceptional tool for identification of chemicals. FTIR patterns wavelengths of OPC, river sand, and coconut husk, such as the bands at 875.68  $\text{cm}^{-1}$ , 993.34  $\text{cm}^{-1}$ , and 3340.71  $\text{cm}^{-1}$  are found in the analysis. It can also be seen that all samples have peaked between 4000 to 500  $\text{cm}^{-1}$ , implying that these materials have different bonds [51].

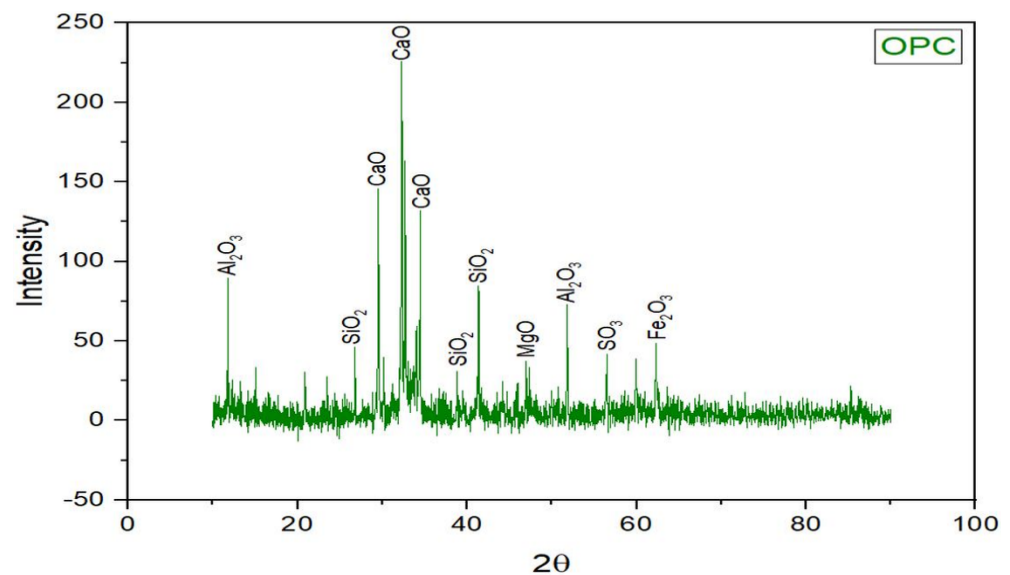


Figure 7. XRD analysis for OPC.

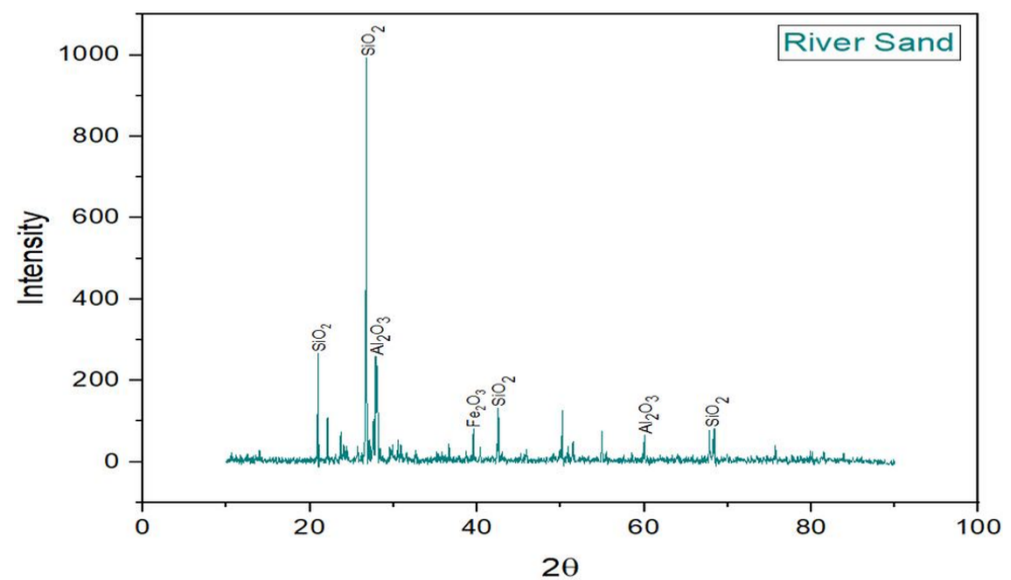


Figure 8. XRD analysis for river sand.

## 6.2. Microstructural Studies on Mortar

This section contains outcomes of the microstructural studies performed on mortar samples made from various mixes utilizing SEM images, EDX, and XRD analyses. Core samples were obtained at the end of various curing durations and analyzed for chemical elements. SEM images, in general, make it difficult to draw recognizable inferences because they primarily provide a pictorial representation of the appearance of the sample. EDX determines the elemental composition by detecting backscattered electrons released from

the examined areas. The strength and durability of hydrated OPC are due to a main nano-crystalline phase called calcium-silicate-hydrate (C-S-H) gel. Because a hydrated sample has other phases, SEM, EDX, and XRD regulate C-S-H phases in a sample. As a result, the results of these studies used to detect C-S-H phases are discussed here.

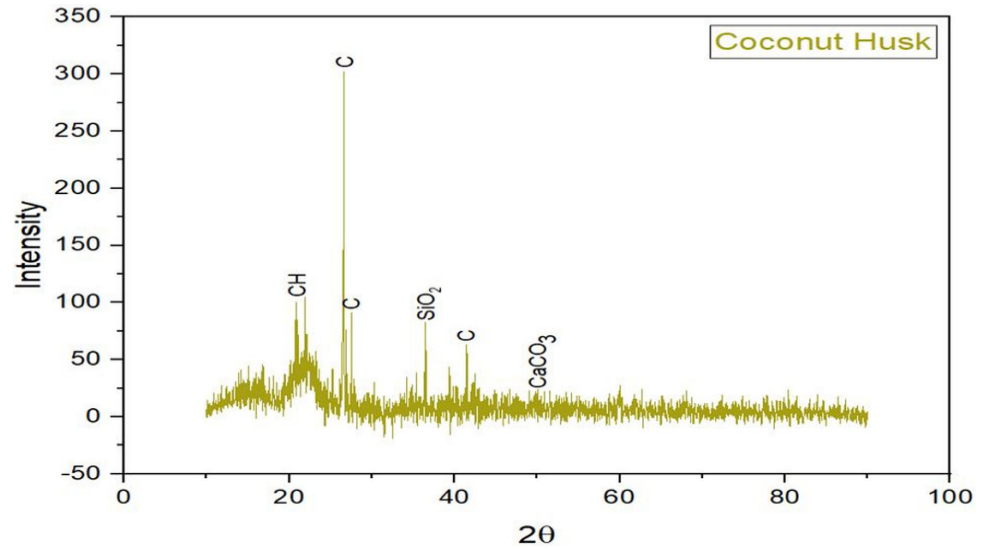


Figure 9. XRD analysis for coconut husk.

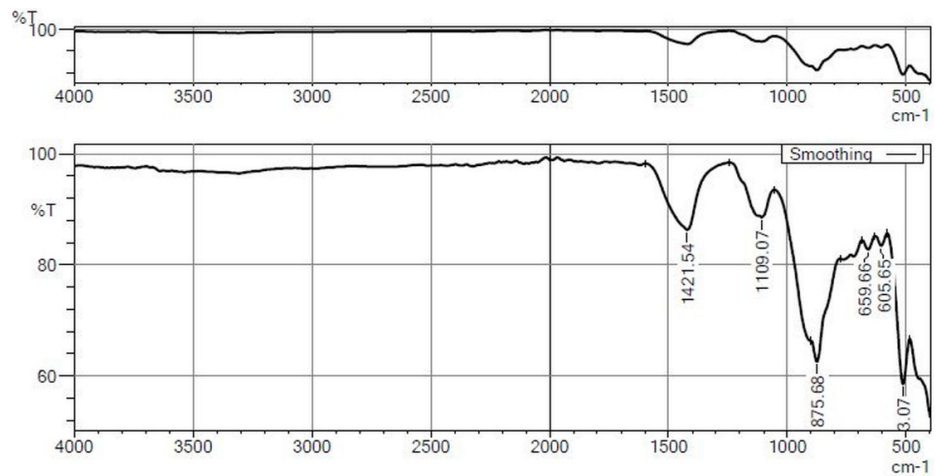


Figure 10. FTIR analysis for OPC.

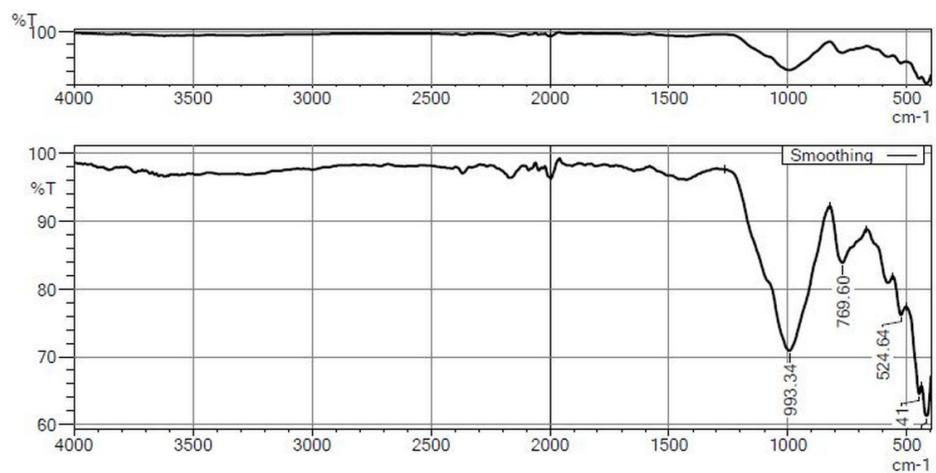


Figure 11. FTIR analysis for river sand.

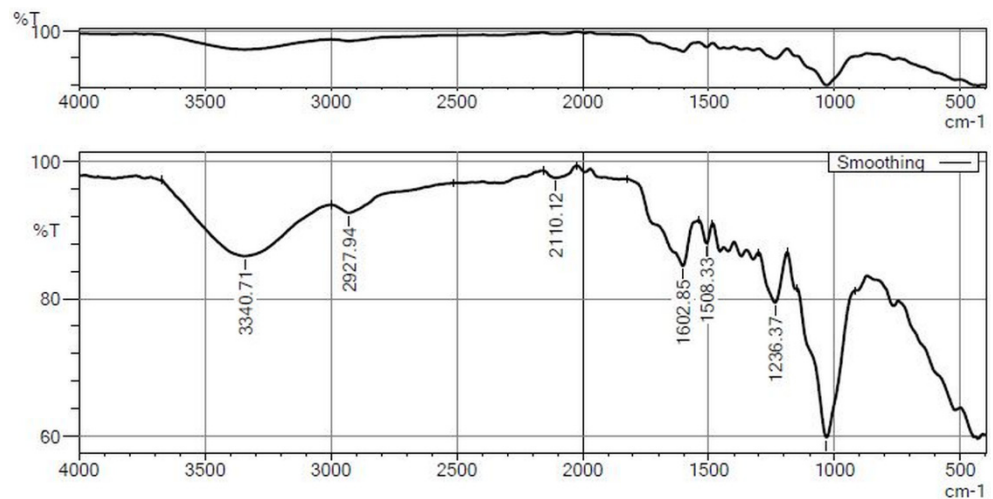
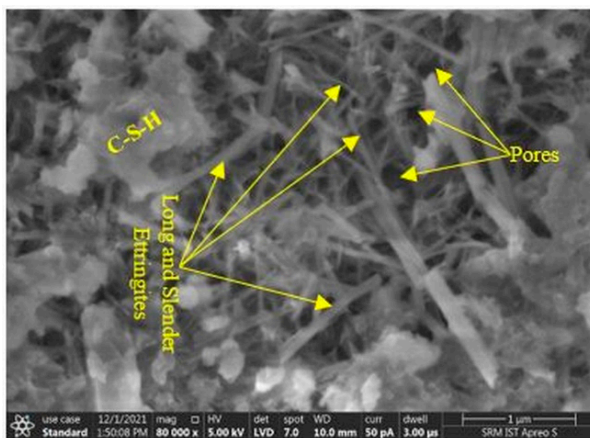


Figure 12. FTIR analysis for coconut husk.

### 6.2.1. SEM Analysis

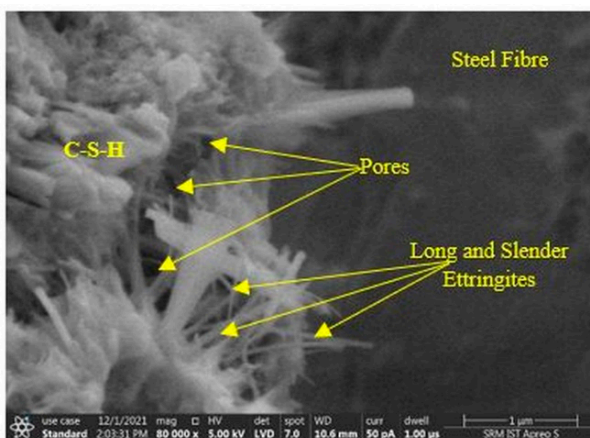
SEM analysis was used to acquire progression images for the samples of CSM, CSSFM, CCHM, and CSCHSFM mixes at ages 0, 1, 3, 7, and 28 days, as shown in Figures 13–17, respectively.



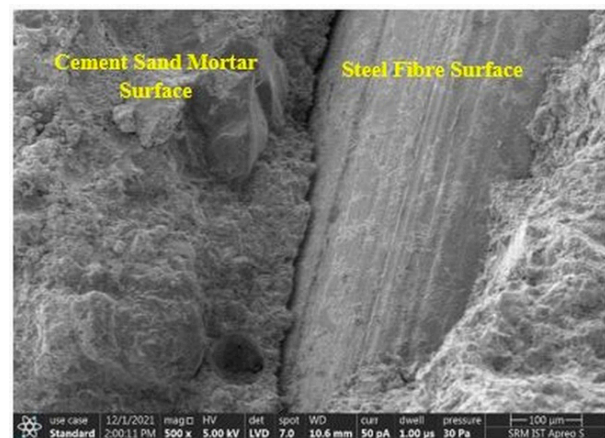
(a) CSM mix



(b) CSM mix at surface level



(c) CSSFM mix



(d) CSSFM mix at surface level

Figure 13. Cont.

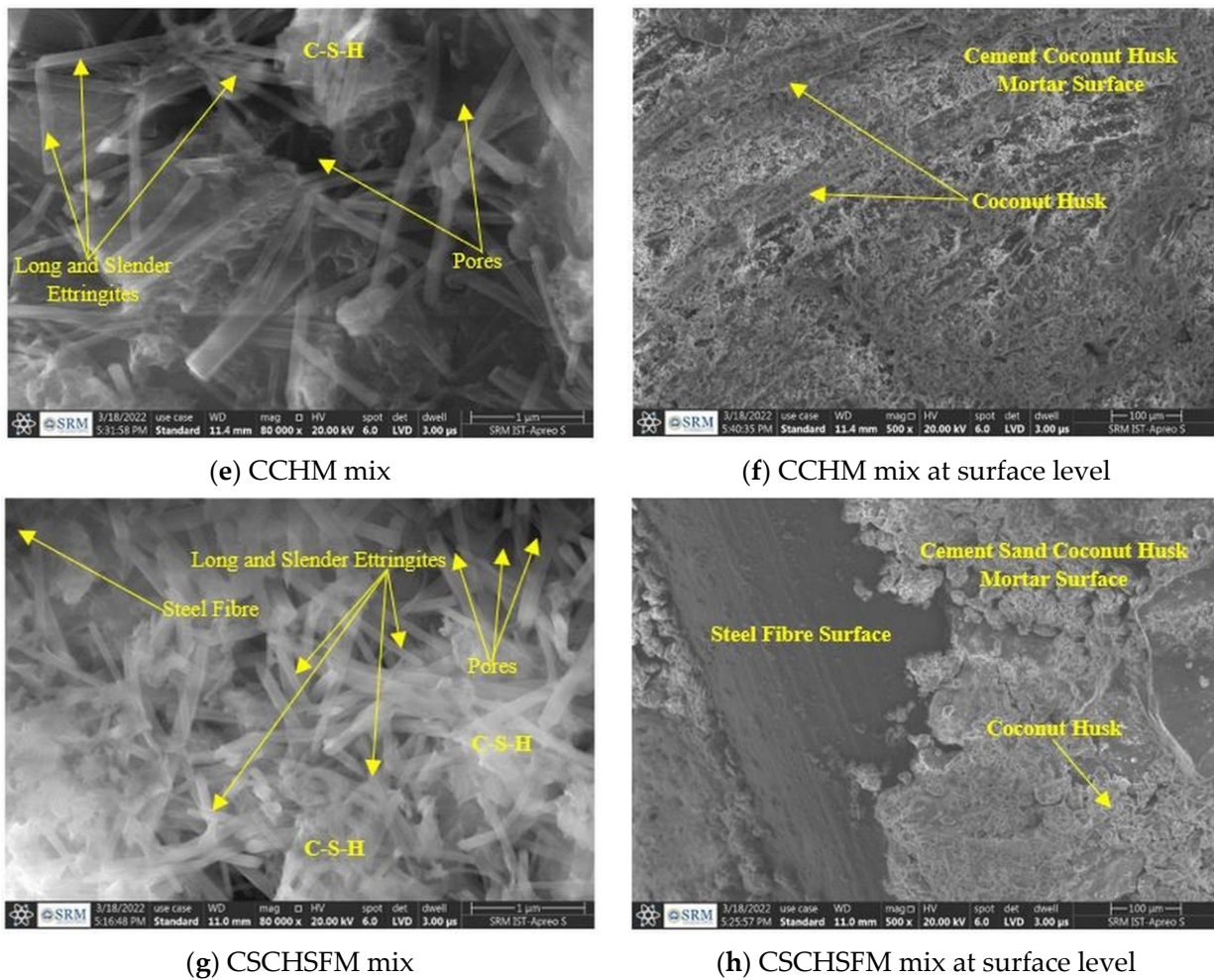


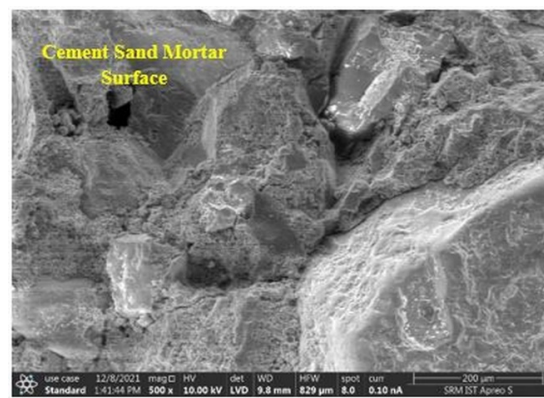
**Figure 13.** SEM images on Day 0 for CSM, CSSFM, CCHM, and CSCHFSM mixes.

Generally, the morphology of C-S-H phase development ranges from weakly crystalline fibres to clusters and reticular networks. When an OPC paste is entirely hydrated, network clusters of C-S-H account for 50–60% of the volume of the solids, which is the most important phase that dictates the paste qualities. Because it only shows clusters and reticular networks and nil ettringite, the C-S-H phase is created in practically the whole area of the images displayed in Figure 17 in this study. All these images (Figures 13–17) reveal that river sand and coconut husk-containing mixes undergo a systematic hydration process. As a result, the standard cement hydration process is unaffected by substituting coconut husk for river sand.

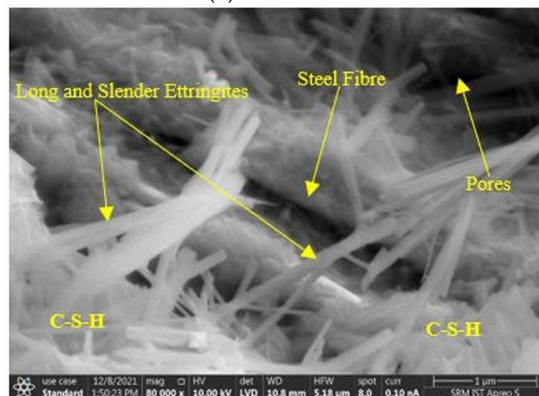
As an effect of the interface between calcium, sulfate, aluminate, and hydroxyl ions, ettringite, which are needle-shaped crystals of calcium tri-sulfoaluminate hydrate, was developed within a few minutes/hours of hydration of the cement. Figures 13 and 14 show ettringite development in four mixes at the early phase of hydration of the cement, which generally consumes the majority of the sulfate in the cement. Ettringite production is the mechanism that governs mortar stiffening. The development of ettringite is frequently connected with peak intensities of Al, S, Si, and Ca in mortar specimens. The early formation of primary ettringite is an important and advantageous constituent of Portland cement systems. Similarly, the long and slender ettringite formed during an earlier phase is converted into aggregations of fibrous crystals, with long prismatic crystals indicating the development of calcium hydroxide (CH), and very slight fibrous crystals indicating the formation of the C-S-H phase, as shown in Figures 15 and 16.



(a) CSM mix



(b) CSM mix at surface level



(c) CSSFM mix



(d) CSSFM mix at surface level



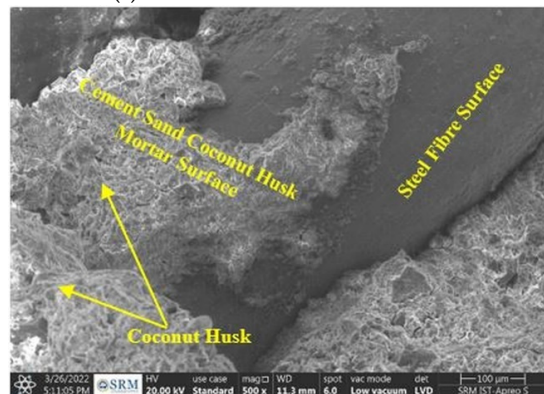
(e) CCHM mix



(f) CCHM mix at surface level

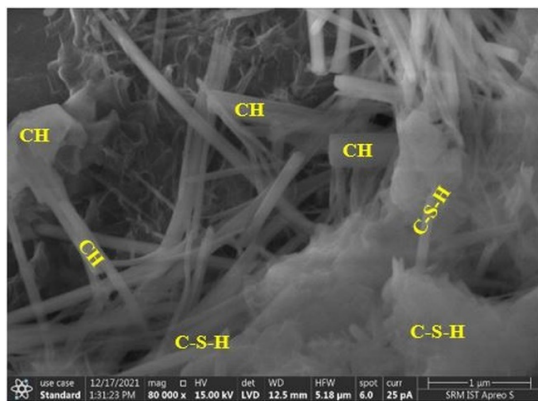


(g) CSCHSFM mix



(h) CSCHSFM mix at surface level

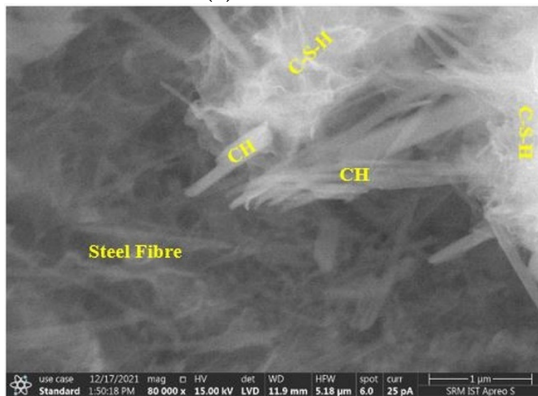
Figure 14. SEM images on Day 1 for CSM, CSSFM, CCHM, and CSCHSFM mixes.



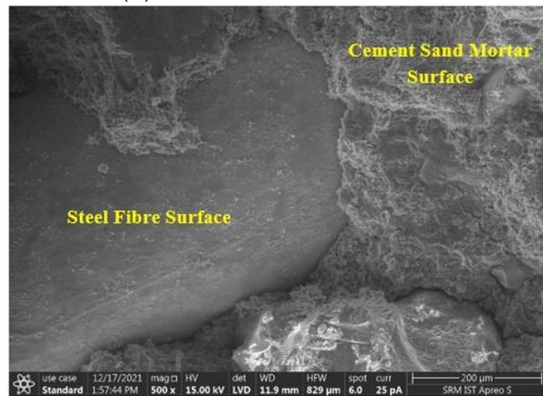
(a) CSM mix



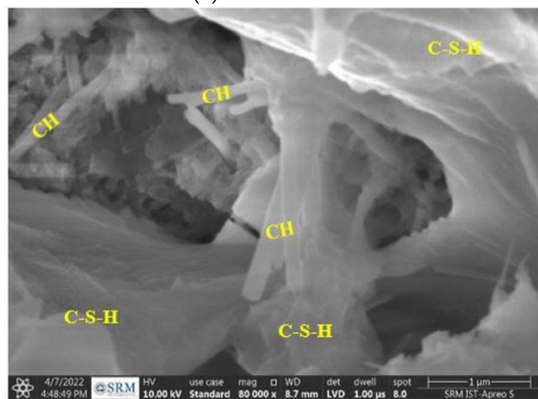
(b) CSM mix at surface level



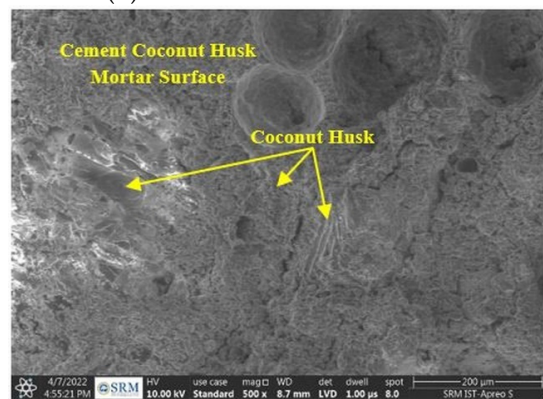
(c) CSSFM mix



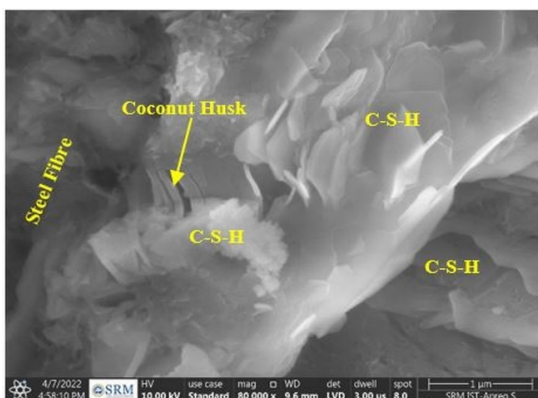
(d) CSSFM mix at surface level



(e) CCHM mix



(f) CCHM mix at surface level



(g) CSCHSFM mix



(h) CSCHSFM mix at surface level

Figure 15. SEM images on Day 3 for CSM, CSSFM, CCHM, and CSCHSFM mixes.

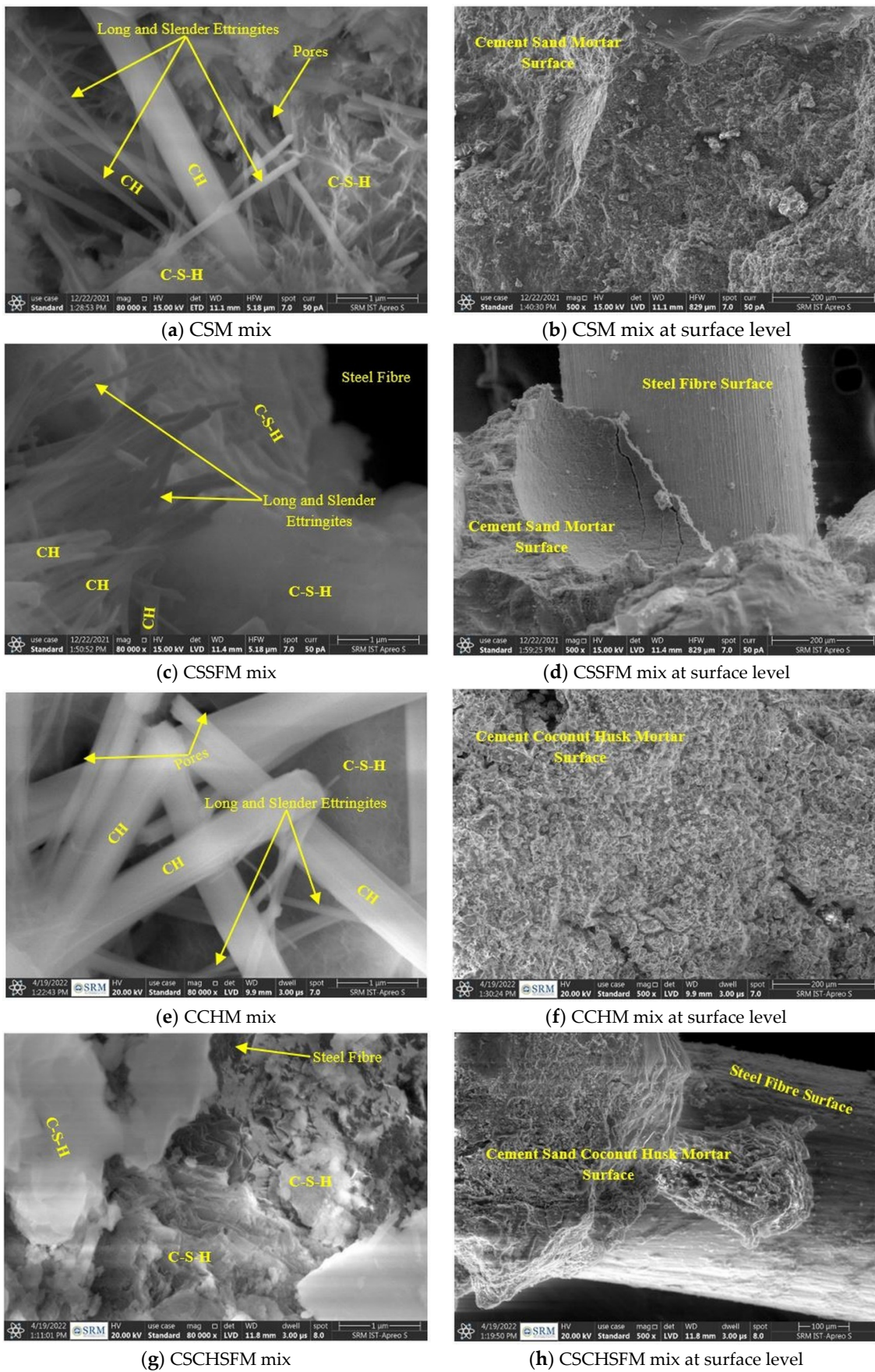


Figure 16. SEM images on Day 7 for CSM, CSSFM, CCHM, and CSCHSFM mixes.

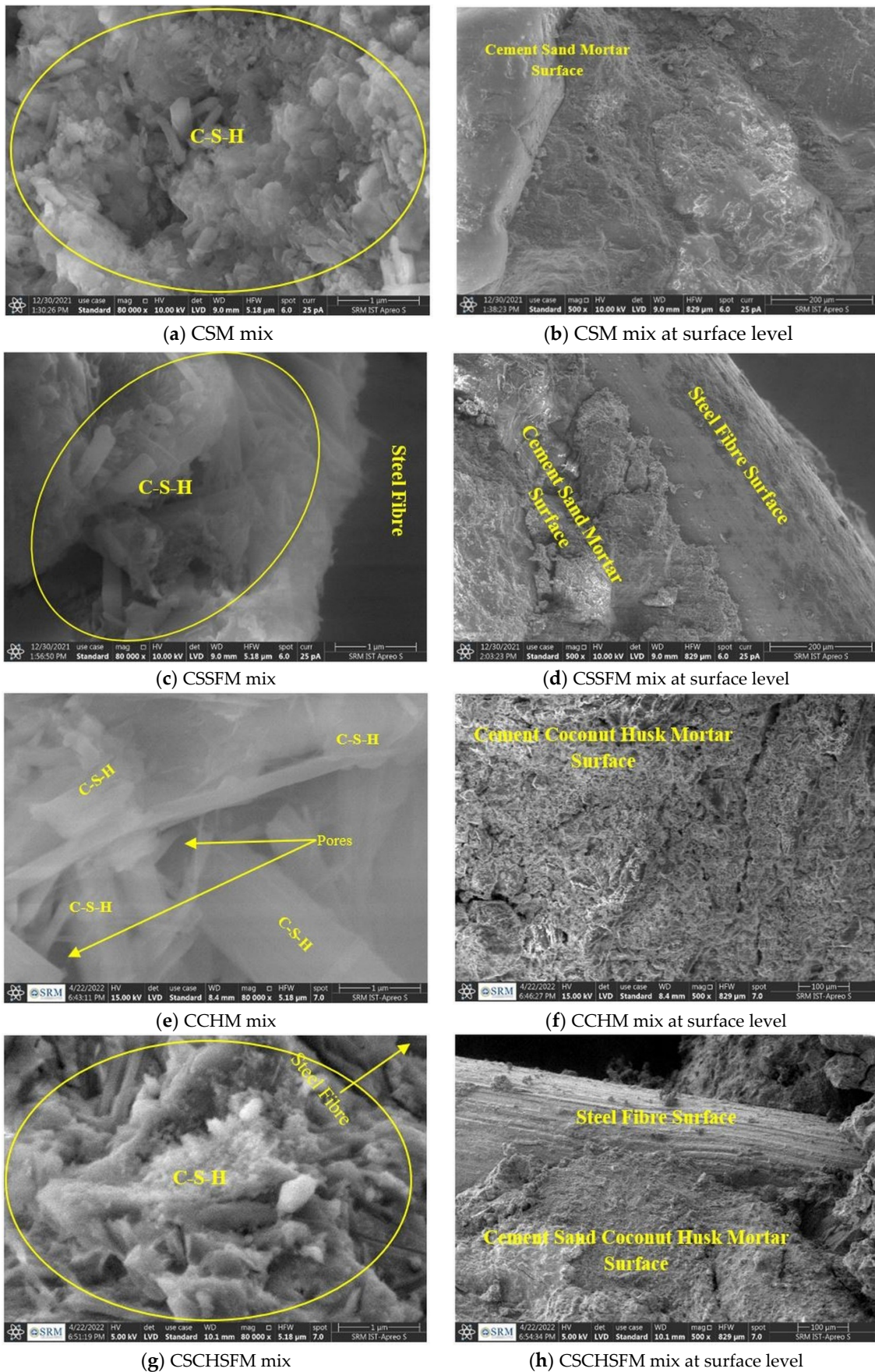


Figure 17. SEM images on Day 28 for CSM, CSSFM, CCHM, and CSCHSFM mixes.

### 6.2.2. EDX Analysis

SEM images of the material should be collected before proceeding with EDX analysis. To obtain the spectra, a target position on this image must be fixed. Using a backscatter electron detector, EDX can be done on the same image to obtain spectra for various spots. Using a combination of SEM and EDX results in spatially distributed elemental studies [52,53]. A data evaluation is required to ascertain the elements contained in the sample spectrum. Each peak in the spectrum represents an element in the complete scan area of the image. For a C-S-H gel to be recognized, three elements—oxygen (O), silica (Si), and calcium (Ca)—must be found. The C-S-H phase is found in areas where Si, Ca, and O are abundant. Furthermore, Ca and O presence is linked to calcium hydroxide (CH)-rich locations. At age 0, 1, 3, 7, and 28 days, EDX was used to attain evolution images for the samples of the four mixes (CSM, CSSFM, CCHM, and CSCHSFM), which are shown in Figures 18–22, respectively.

At the moment of analysis, an automatic table of atomic counts (in percentages) is usually produced, from which the Ca:Si ratio can be determined. The EDX analysis indicates that the amounts of C-S-H in all four mixes at various ages are affected by pozzolanic reactions. A lower atomic Ca:Si proportion indicates that a large portion of the cement was retorted with portlandite. Because C-S-H is hyphenated and not a definite molecule, the Ca:Si ratio for the well-hydrated C-S-H phase is estimated to be between 1.5 and 2.0 in the literature [54,55]. Table 4 shows the Ca:Si ratios of several blends from this investigation at various ages.

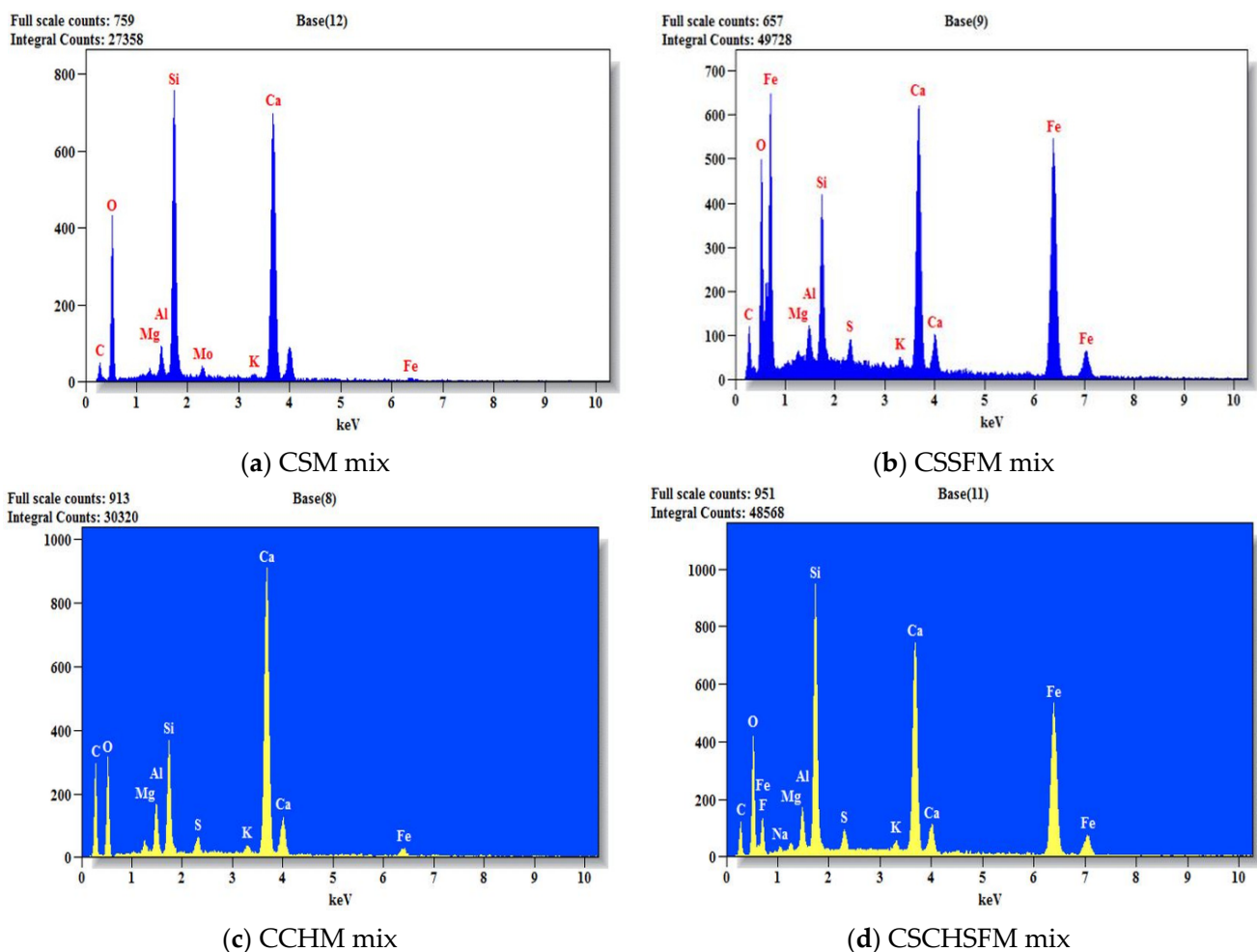


Figure 18. EDX analysis on Day 0 for CSM, CSSFM, CCHM, and CSCHSFM mixes.

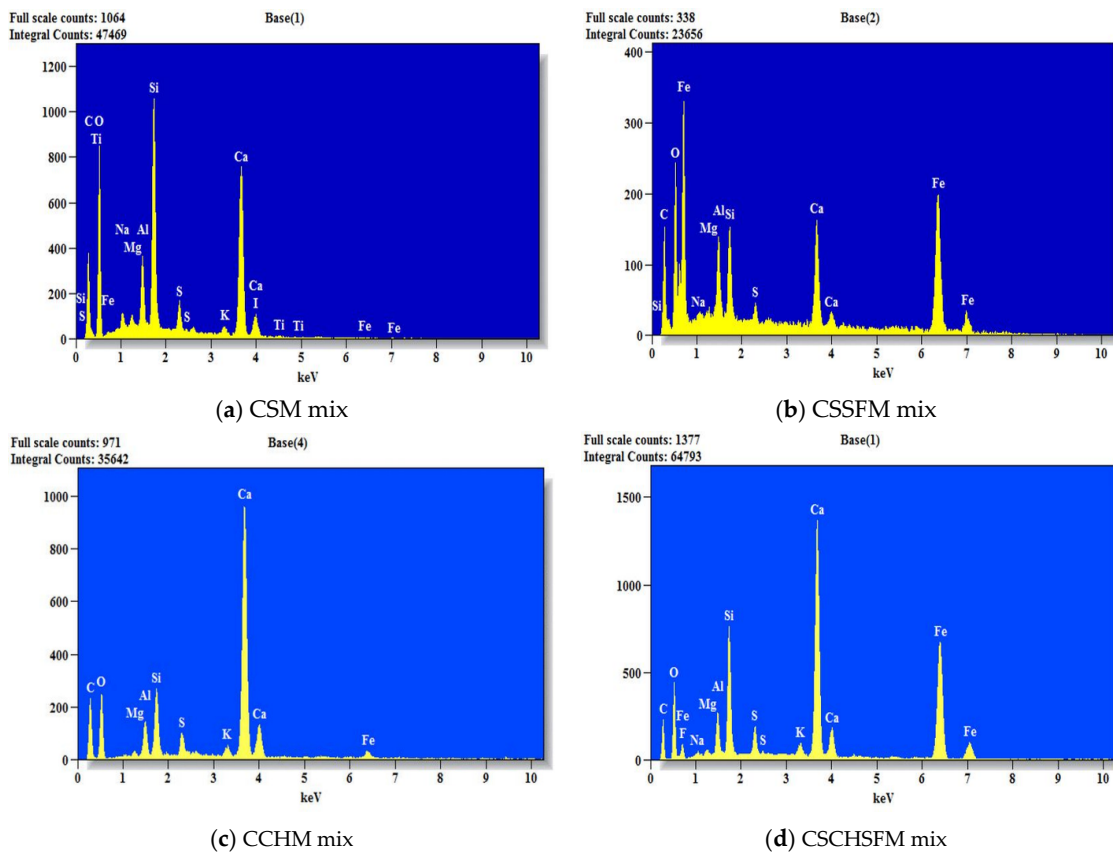


Figure 19. EDX analysis on Day 1 for CSM, CSSFM, CCHM, and CSCHSFM mixes.

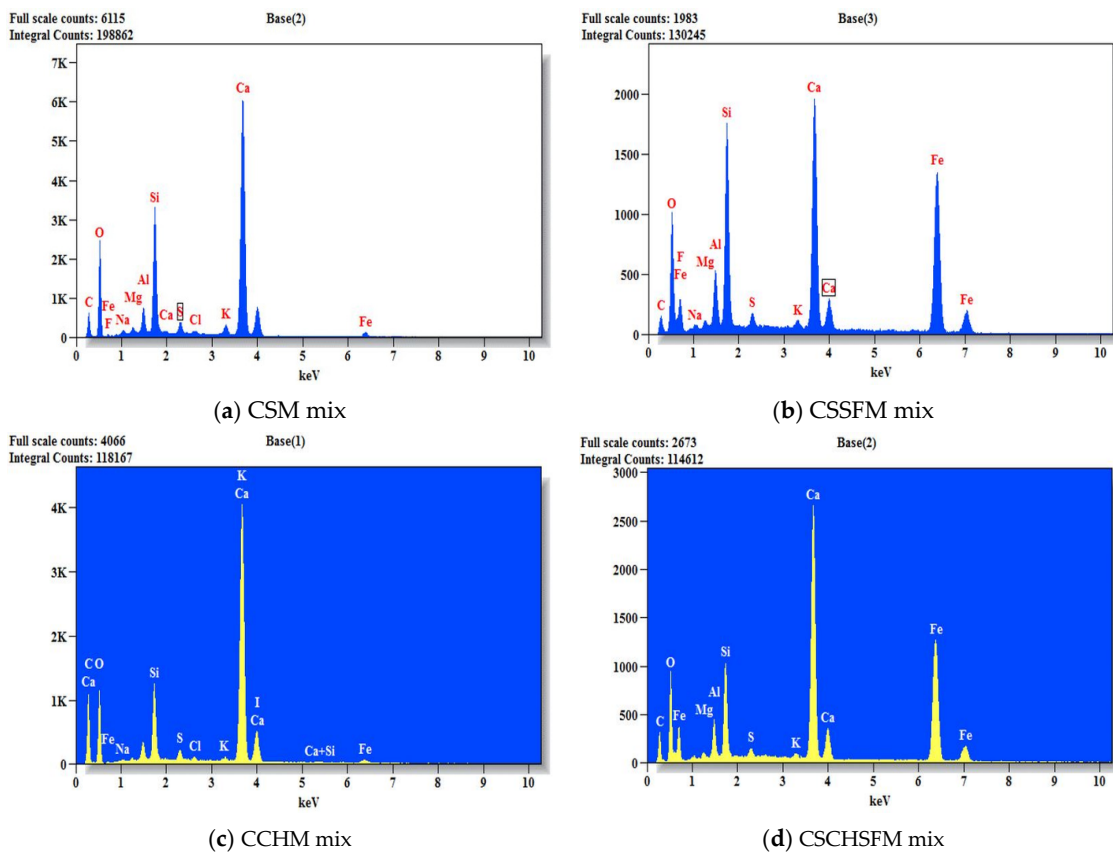


Figure 20. EDX analysis on Day 3 for CSM, CSSFM, CCHM, and CSCHSFM mixes.

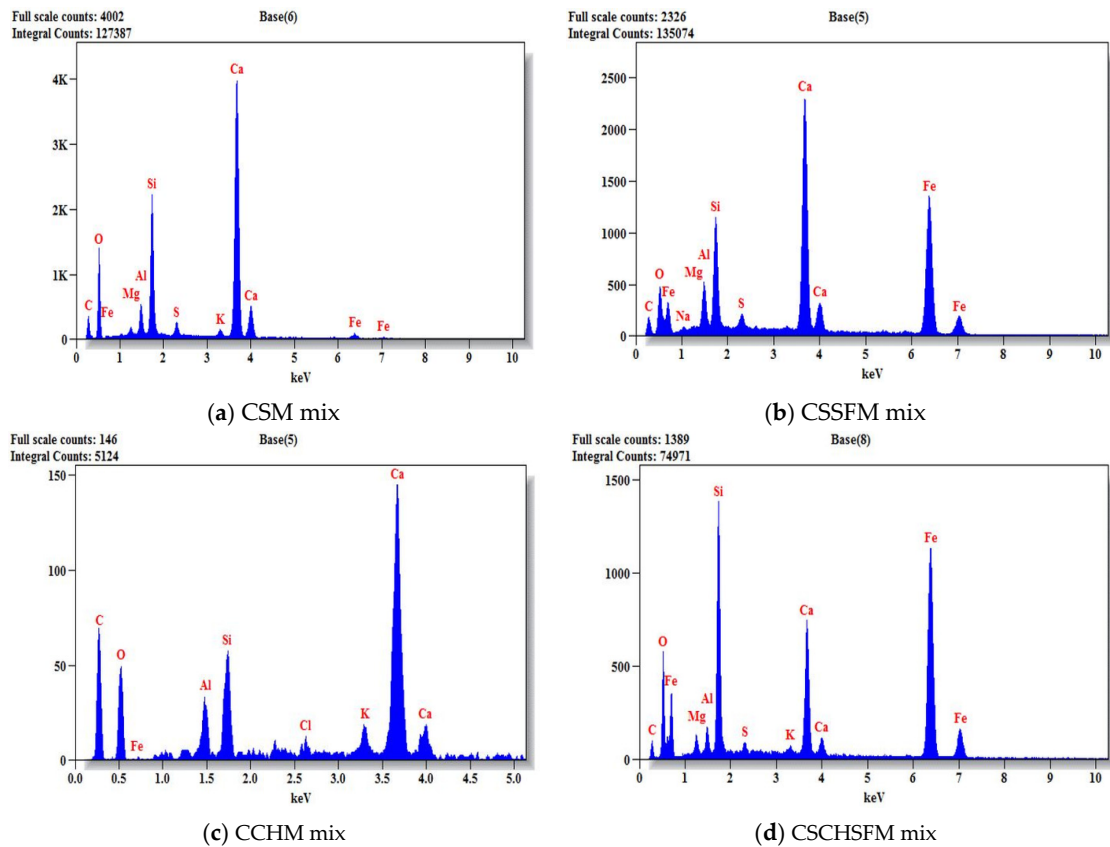


Figure 21. EDX analysis on Day 7 for CSM, CSSFM, CCHM, and CSCHSFM mixes.

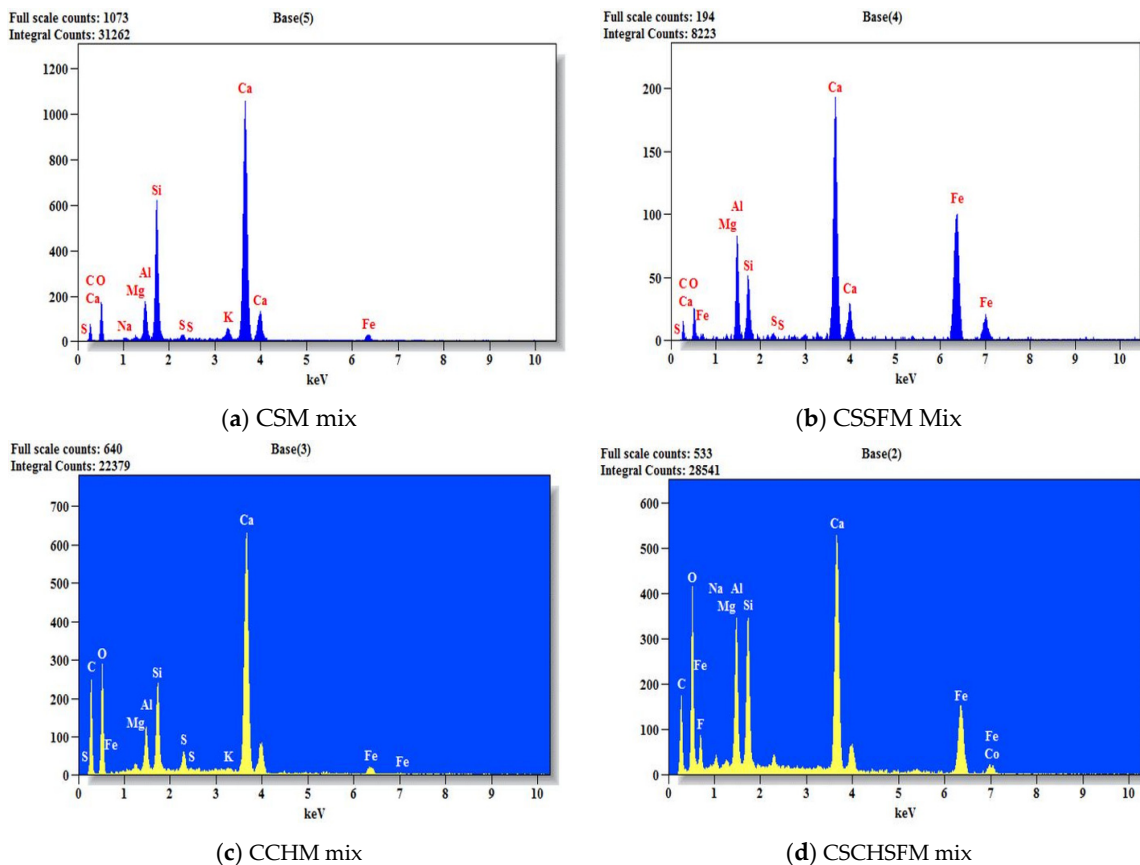


Figure 22. EDX analysis on Day 22 for CSM, CSSFM, CCHM, and CSCHSFM mixes.

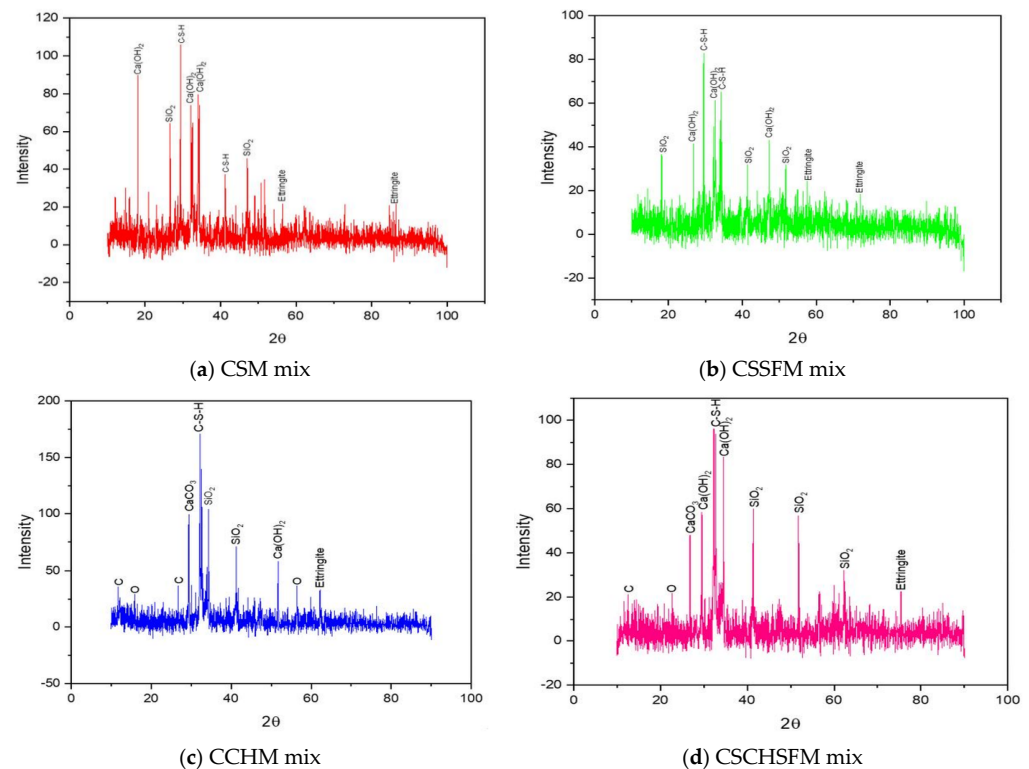
**Table 4.** Ratio (Ca:Si) for different mixes on different days.

Mixes	Ratio (Ca:Si)				
	Day 0	One Day 1	Day 3	Day 7	Day 28
CSM	2.42	2.35	1.87	1.58	1.38
CSSFm	2.36	2.07	1.98	1.95	1.12
CCHM	2.48	2.29	2.01	1.85	1.78
CSCHSFm	2.23	1.96	1.89	1.40	1.27

The Ca:Si ratio is larger in the early days and decreases with age, as seen in Table 4. At 28 days, the Ca:Si ratio for all mixes is between 1.0 and 2.5, with CSM and CCHM demonstrating a higher Ca:Si ratio than CSSFM and CSCHSFm, emphasising that the methodical hydration process happens in both river sand and coconut husk containing mixes.

### 6.2.3. XRD Analysis

Analysis using X-ray diffraction was performed on samples CSM, CSSFM, CCHM, and CSCHSFm at ages 0, 1, 3, 7, and 28 days, and the results are shown in Figures 23–27 [56], respectively. The purpose of these analyses was to investigate the phase nature of these materials and to identify the primary reacting compounds, which include ettringite, C-S-H,  $\text{Ca}(\text{OH})_2$ , and calcium hydroxide (CH) as the primary chemicals that can be identified by XRD. Table 5 shows that the intensity of the C-S-H peaks has increased while the strength of the rest of the peaks has decreased. Table 5 shows that the intensity of the C-S-H peaks has increased while the strength of the rest of the peaks has decreased. Table 5 presents the intensity count ranges for the C-S-H,  $\text{Ca}(\text{OH})_2$ , and ettringite compounds. These ranges are shown for each of the four mixes at varying ages. The intensity counts of the C-S-H compounds are high compared to the formation of the  $\text{Ca}(\text{OH})_2$  compounds. This demonstrates no interruption of the pozzolanic reactions, which in turn has a substantial positive effect on the reduction of  $\text{Ca}(\text{OH})_2$ -(CH) in all of the mixes, which is advantageous for the quality of mortar strength.

**Figure 23.** XRD analysis on Day 0 for CSM, CSSFM, CCHM, and CSCHSFm mixes.

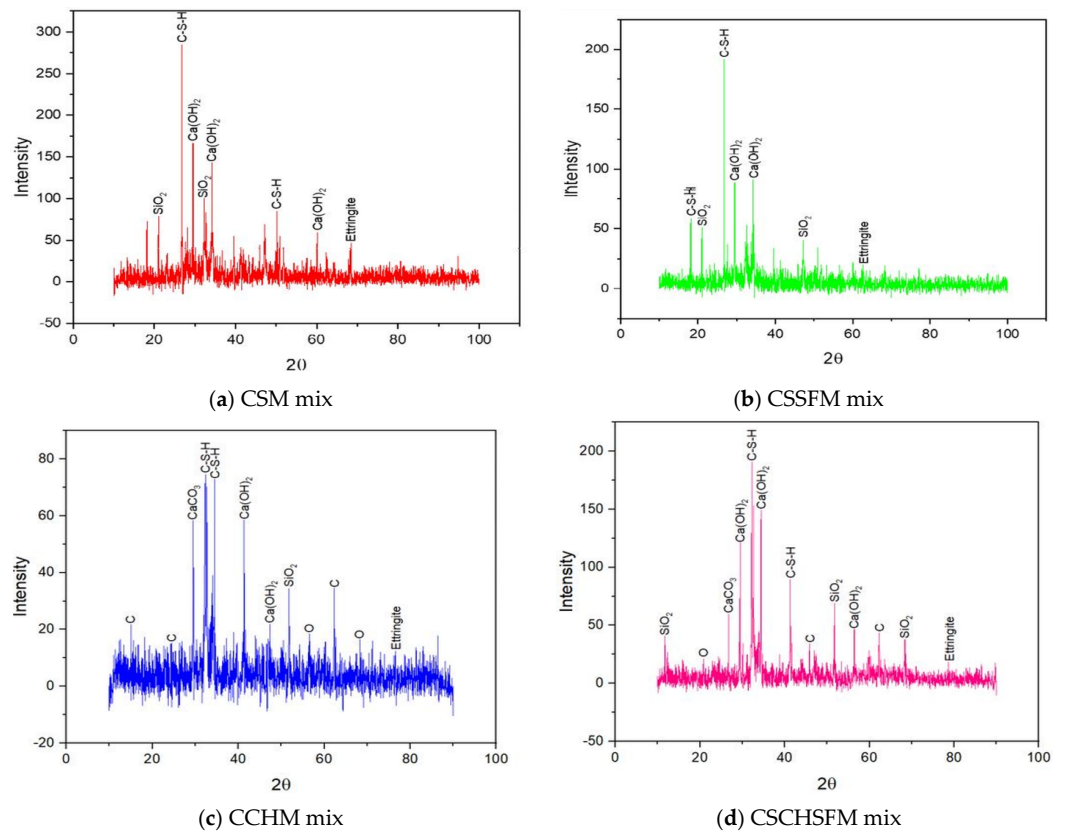


Figure 24. XRD analysis on Day 1 for CSM, CSSFM, CCHM, and CSCHSFM mixes.

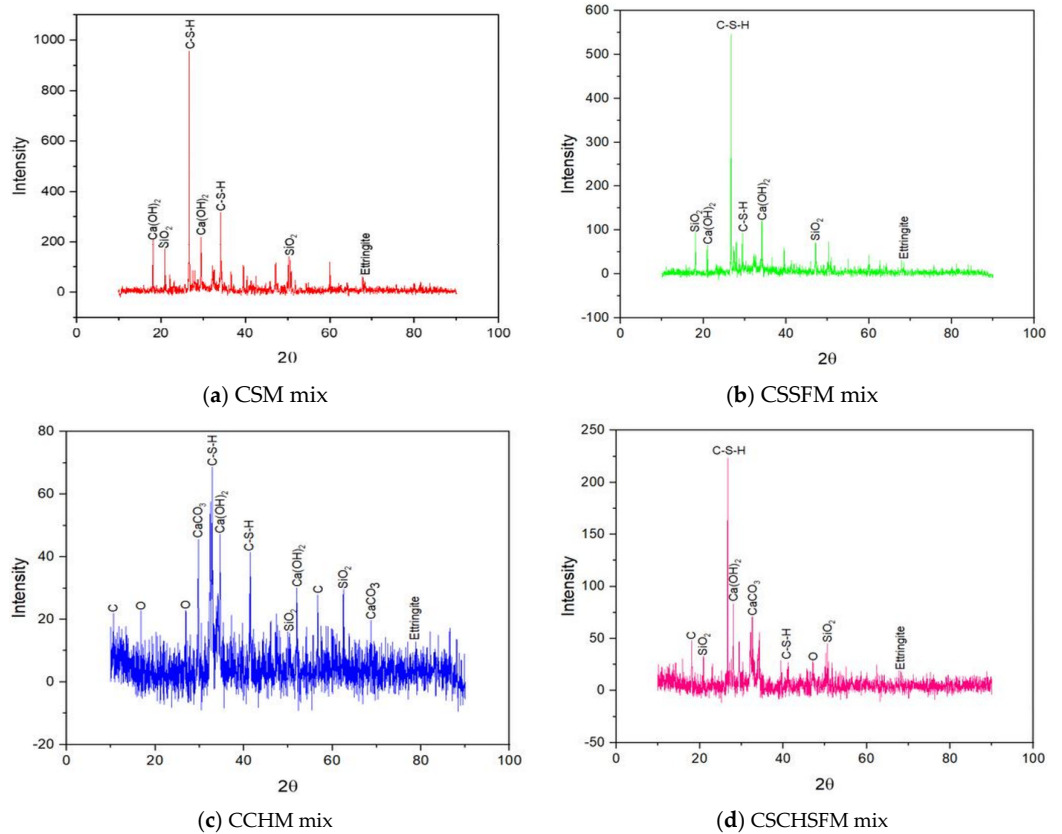


Figure 25. XRD analysis on Day 3 for CSM, CSSFM, CCHM, and CSCHSFM mixes.

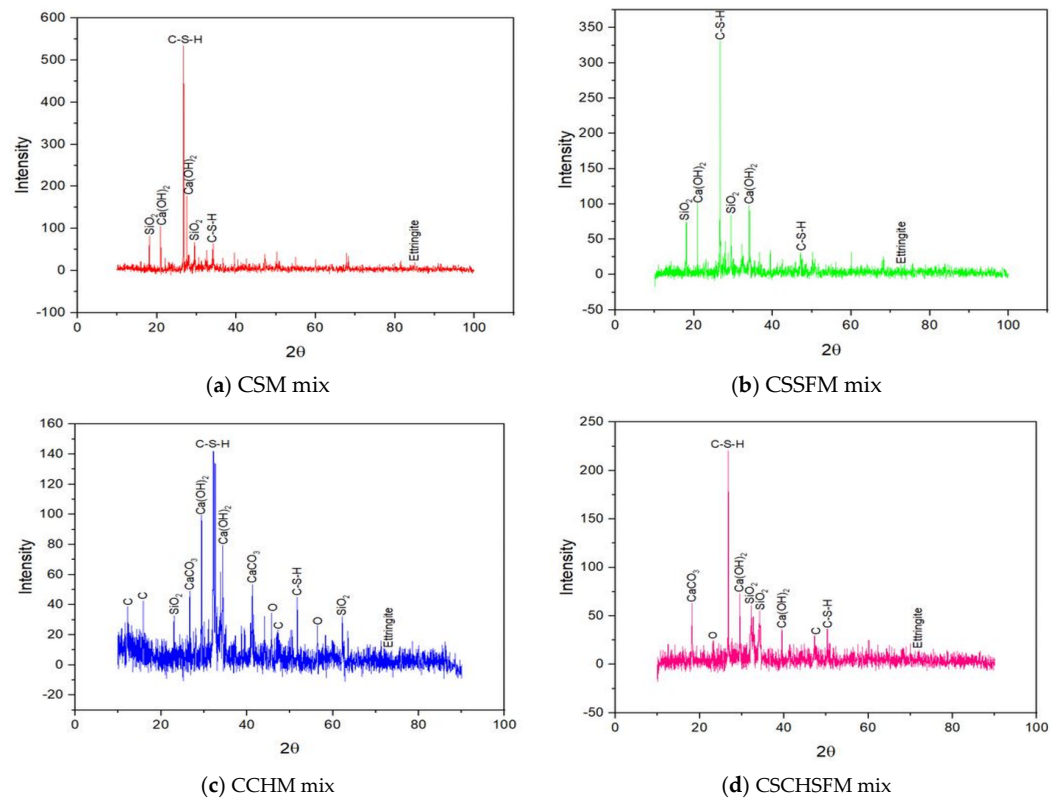


Figure 26. XRD analysis on Day 7 for CSM, CSSFM, CCHM, and CSCHSFM mixes.

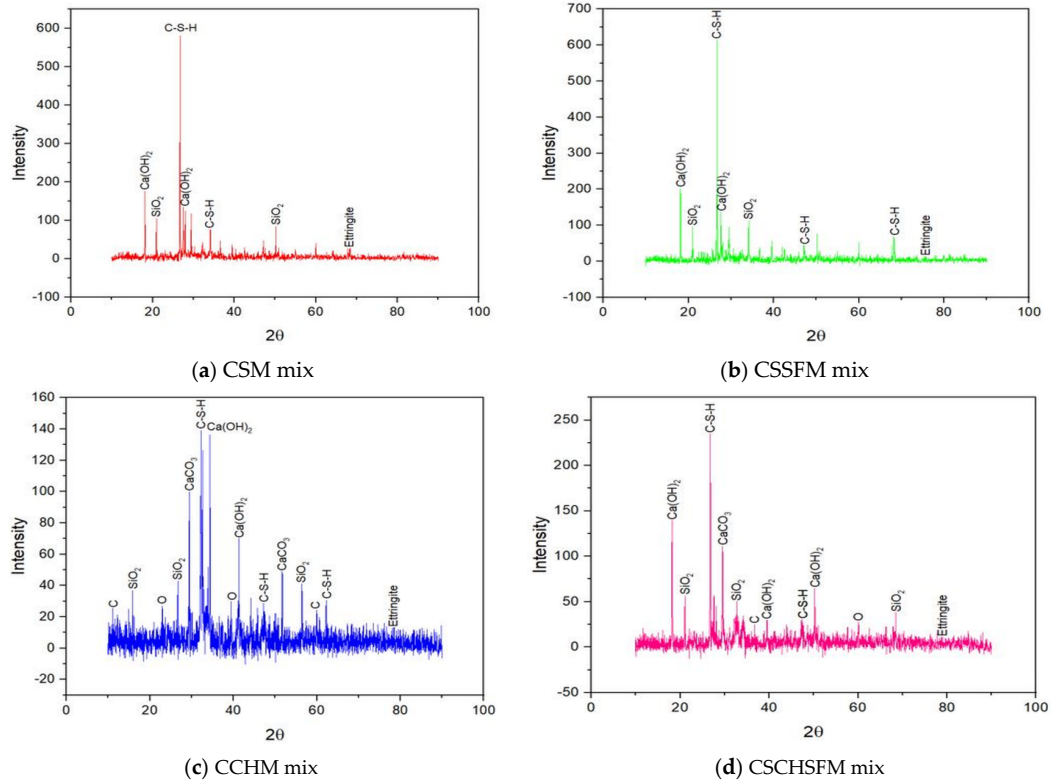


Figure 27. XRD analysis on Day 28 for CSM, CSSFM, CCHM, and CSCHSFM mixes.

### 6.3. Fresh Mortar Properties

True slump patterns were obtained for all the mixes that did not experience any segregation; hence, it can be stated that using coconut husk in place of river sand results

in cohesive mixes. Slump values of 30 mm for the CSM mix, 10 mm for the CSSFM mix, 40 mm for the CCHM mix, and 20 mm for the CSCHSFM mix were measured. The values from the flow table test were measured as 101.67% for the CSM mix, and 101.3% for the CCHM mix, which is close to the requirement of IS 4031(Part 7)-1988 [57] (i.e.,)  $110 \pm 5\%$ . However, these values are 64.3% for the CSSFM mix, and 27.7% for the CSCHSFM mix, which did not satisfy the requirement of IS 4031(Part 7)-1988 [57]. Since this IS code recommendation is meant for conventional mortar and for fibre-added mortar, it cannot be taken for comparison and validation of the results. In general, from these results, the workability of the mortar mixes can be stated as a medium degree of workability, when the flow value is considered [58,59].

**Table 5.** Maximum intensity of compounds from XRD.

Compounds (Peak Intensity)	Day 0	Day 1	Day 3	Day 7	Day 28
	<b>CSM Mix</b>				
C-S-H	100–120	250–300	900–1000	500–600	500–600
Ca(OH) <sub>2</sub>	60–80	150–200	200–300	150–200	100–200
Ettringite	20–40	25–50	0–10	0	0
<b>CSSF M Mix</b>					
C-S-H	80–100	100–200	500–600	300–350	600–700
Ca(OH) <sub>2</sub>	60–70	50–100	100–150	50–100	200–300
Ettringite	10–20	10–50	0–10	0	0
<b>CCHM Mix</b>					
C-S-H	150–200	70–80	70–80	140–160	140–160
Ca(OH) <sub>2</sub>	50–100	50–60	40–50	100–120	120–140
Ettringite	25–50	10–20	10–20	10–20	0–10
<b>CSCHSF M Mix</b>					
C-S-H	90–100	150–200	200–250	200–250	200–250
Ca(OH) <sub>2</sub>	80–90	100–150	50–100	50–100	100–150
Ettringite	20–30	0–50	0–25	0–10	0

Both CCHM and CSCHSFM mixes generated with coconut husk have lower workability than river sand-containing mortar mixes. However, their slump values are more comparable to CSM and CSSFM mixes. This is because coconut husk typically has a much higher water absorption rate (20–25%) as the parent material of coconut husk is wood (Coconut shell), compared to river sand. The fresh density of each mortar mixture is measured as 2210 kg/m<sup>3</sup> for the CSM mix, 2285 kg/m<sup>3</sup> for the CSSFM mix, 1360 kg/m<sup>3</sup> for the CCHM mix, and 2150 kg/m<sup>3</sup> for the CSCHSFM mix, respectively. While comparing the fresh density of the CCHM mix with the CSM mix, the CCHM mix density is reduced to 38.5%. The fresh density of the CSCHSFM mix is compared with the CSSFM mix, and it is decreased by 5.9%. From this study, the coconut husk mixed mortar used is reduced when compared to the river sand mortar mix used because the coconut husk is less dense than river sand.

#### 6.4. Hardened Mortar Properties

The hardened properties of four different mortars (CSM, CSSFM, CCHM, and CSCHSFM) are presented in Table 6. After 28 days, the hardened density of the CCHM mix is compared to the CSM mix, which is reduced to 37.7%. The CSCHSFM mix is compared to the CSSFM mix, which is decreased to 6.84%. The hardened density of all four mixes increases with the increase in age since the enhancement of the pozzolanic reaction of cementitious materials takes place through the conversion of long and slender ettringite into the large prismatic

crystal of calcium hydroxide (CH), into short fibrous crystals (C-S-H), and then into close clusters and a reticular network due to C-S-H creation in the later stage, which decreases the presence of pores. This is demonstrated by the SEM analysis covered in Section 6.2.1. Using coconut husk as a fine aggregate in mortar reduced the self-weight of the mortar by approximately 60% compared to the river sand mortar used. Therefore, it can be considered a lightweight mortar [60,61].

**Table 6.** Hardened mortar properties of mixes used.

Test Age	CSM Mix		CSSFM Mix		CCHM Mix		CSCHSFM	
	Density (kg/m <sup>3</sup> )	Strength (N/mm <sup>2</sup> )	Density (kg/m <sup>3</sup> )	Strength (N/mm <sup>2</sup> )	Density (kg/m <sup>3</sup> )	Strength (N/mm <sup>2</sup> )	Density (kg/m <sup>3</sup> )	Strength (N/mm <sup>2</sup> )
Day 3	2260	23.20	2295	28.45	1385	2.35	2170	22.15
Day 7	2275	28.35	2310	35.30	1390	2.60	2175	29.50
Day 28	2310	37.00	2340	40.25	1440	5.90	2180	36.10

In the application of ferrocement, river sand is replaced by coconut husk to produce environment-friendly components. According to ACI codes [37,38] and the WRD handbook [39], the CSM, CSSFM, and CSCHSFM mixes attained the target compressive strength of 35 N/mm<sup>2</sup>, except for the CCHM mix. The ratio of 1:3 was adopted for this study, and the appropriate level of strength was reached for the CSM and CSSFM mixes. Though the 1:3 ratio was adopted for the CCHM mix, it resulted in just 17% of the target strength. Therefore, as per the trials, a CSCHSFM mix was used in combination with 40% coconut husk, 60% river sand, and 6% steel fibre to obtain the desired level of strength.

#### 6.4.1. Mechanical Properties

Table 7 shows the testing results of the mechanical properties including splitting tensile and flexural strength and impact resistance.

**Table 7.** Mechanical properties of mixes used.

Test Age	CSM Mix		CSSFM Mix		CCHM Mix		CSCHSFM Mix	
	Splitting Tensile Strength (N/mm <sup>2</sup> )							
Day 3	2.29		4.17		0.67		1.85	
Day 7	2.51		4.39		0.95		2.45	
Day 28	4.48		5.65		1.36		3.23	
Flexural Strength (N/mm <sup>2</sup> )								
Day 3	14.76		18.83		13.90		15.36	
Day 7	18.77		22.93		16.67		20.97	
Day 28	22.46		25.29		17.19		23.10	
Impact Resistance in Joules								
	Initial Crack	Final Crack	Initial Crack	Final Crack	Initial Crack	Final Crack	Initial Crack	Final Crack
Day 3	159	199	318	497	80	159	179	358
Day 7	298	338	656	855	119	199	338	557
Day 28	398	438	1353	1870	179	239	358	597

#### 6.4.2. Splitting Tensile Strength

The splitting tensile strength of the Day 28 results of the CSCHSFM mix is 3.23 N/mm<sup>2</sup> (8.95% of its compressive strength), representing a decrease of 27.90% and 42.83% when

compared to the CSM and CSSFM mix. The CCHM mix is  $1.36 \text{ N/mm}^2$  (23% of its compressive strength), which is 69.6% lower than the CSM mix; and the CSCHSFM mix is 57.90% higher than the CCHM mix. Similarly, the CSSFM mix is  $5.65 \text{ N/mm}^2$  (14% of its compressive strength), which increased by 26.12% more than the CSM mix. Based on the findings of this study on splitting tensile strength, it is concluded that the CSCHSFM mix showed a similar performance compared to the CSM and CSSFM mixes.

#### 6.4.3. Flexural Strength

The flexural strength of the Day 28 results of the CSCHSFM mix is  $23.10 \text{ N/mm}^2$  (63.9% of its compressive strength), which decreased by 8.66% compared to the CSSFM mix ( $25.29 \text{ N/mm}^2$ ). The flexural performance of the CCHM mix is  $17.19 \text{ N/mm}^2$ , which is higher than compressive strength ( $5.90 \text{ N/mm}^2$ ) due to the fibrous nature of coconut husk. Similarly, the flexural strength of the CSSFM mix is  $25.29 \text{ N/mm}^2$  (62.83% of its compressive strength), which increased by 12.6% compared to the CSM mix. However, in the case of the CCHM and CSCHSFM mixes, it is slightly higher than compressive strength (30% to 65%) due to the fibrous nature of coconut husk. In the presence of 6% crimped steel fibres in the CSSFM and CSCHSFM mixes, a certain amount of coconut husk in the CSCHSFM mixes can have better flexural strength than the CSM and CCHM mixes.

#### 6.4.4. Impact Resistance

Regarding the impact resistance on Day 28, the initial crack resistance of the CSM mix is 398 joules (20 blows), and the final crack resistance is 438 joules (22 blows). Similarly, the impact resistance of the CSSFM mix is 1353 joules (68 blows) for the initial crack and 1870 joules (94 blows) for the final crack. Likewise, the initial crack resistance of the CCHM mix is 179 joules (9 blows), whereas the final crack resistance is 239 joules (12 blows). The impact resistance of the CSCHSFM mix is 358 joules (18 blows) for the initial crack and 597 joules (30 blows) for the final crack. The CSSFM and CSCHSFM mixes contain 6% crimped steel fibres, which improve the impact resistance in both the initial and final cracking compared to the CSM and CCHM mixes. As a result, the mortar mixes of CSM, CSSFM, and CSCHSFM mixes can be used for structural elements and the CCHM mix can be used for non-structural elements. Figures 28 and 29 illustrate the impact resistance in joules for initial cracking and final cracking at various ages (3, 7, and 28 days) of the mortar mixes, respectively.

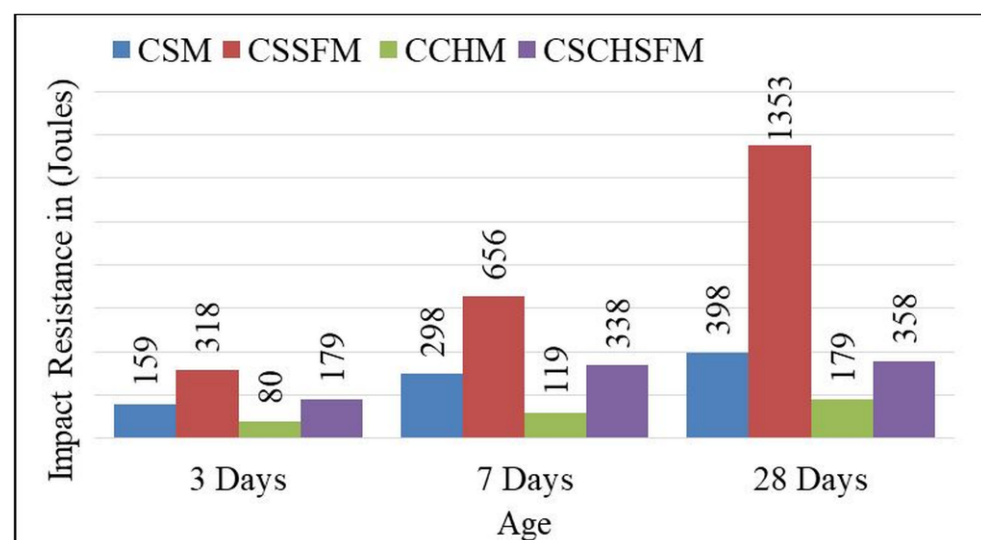


Figure 28. Impact resistance of mortar mixes at initial failure.

Table 8 compares the characteristics of river sand and coconut husk in order to show the findings of this study for the benefit of the reader.

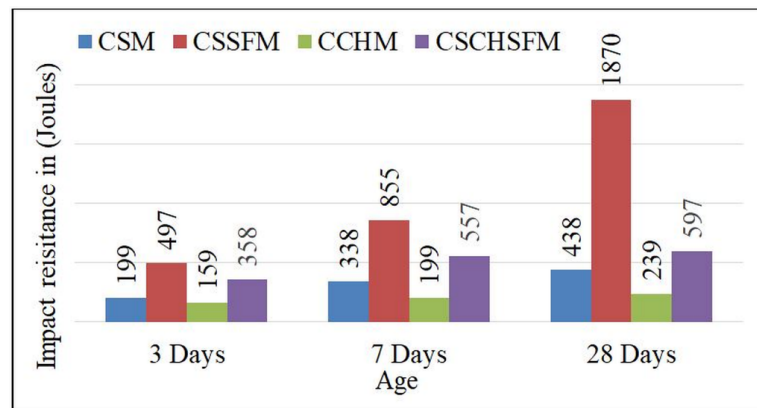


Figure 29. Impact resistance of mortar mixes at final failure.

Table 8. Comparison of river sand and coconut husk characteristics.

Characteristics	River Sand	Coconut Husk
Surface structure	Smooth texture	Rough texture
Oversizing	It cannot be avoided	Can be avoided
FTIR pattern		Different patterns
Bonding nature		Different patterns
Cement hydration processes		Not affected
Ratio (Ca:Si) at 28 days for mortar	1.38	2.24
Workability	Increases	Decreases
Mortar density	More	Less
Mortar strength	More	Less

Using coconut husk as a fine aggregate in mortar production has similar microstructural properties and results in traditional mortar behaviour (CSM). This has advantages because these two mixes (CCHM and CSCHSFM) are innovative and made from environmental waste resources generated from the agriculture sector. Therefore, coconut husk can be considered as a sustainable alternate material. The compressive, split tensile, and flexural strength, and impact resistance of the mortar made with coconut husk and steel fibre in the CSCHSFM and CSSFM mixes are higher than other mixes that used river sand and without steel fibre in the CSM and CCHM mixes. The mechanical properties have been studied in depth, but other important aspects, such as bonding, cracks, and deflection characteristics, need to be examined further to arrive at definitive conclusions about the advantages of ferrocement structural elements.

For the benefit of the readers, the coconut husk used and fresh mortar (CCHM and CSCHSFM) are shown in Figure 30.



Figure 30. Fresh mortar (a) CCHM and (b) CSCHSFM.

## 7. Conclusions

Coconut husk is an alternative fine aggregate that can be utilized in place of river sand, which in turn can be used for mortar production. Since it has a lesser density, which has been proven to be an advantage for developing lightweight mortar, it can be used for ferrocement applications.

Through FTIR analysis it was found that the primary IR band of river sand and coconut husk are located between 4000 to 500  $\text{cm}^{-1}$ , but the wavelength of bands are different, indicating that both materials have different bonds and chemical structures. Additionally, a methodical hydration process was found through SEM analysis of CSM, CSSFM, CCHM, and CSCHSFM mix for 0, 1, 3, 7, and 28 days. Therefore, it is possible to suggest that substituting coconut husk for river sand does not affect the process of conventional cement hydration. At 28 days, the Ca:Si ratio for all four mixes is between 1.0 to 2.5, with CSM and CCHM mixes having a higher Ca:Si ratio than CSSFM and CSCHSFM mixes. This demonstrates and emphasizes that the systematic hydration process has taken place in mixes containing river sand and coconut husk, as noted in the EDX analysis. The results of CSM, CSSFM, CCHM, and CSCHSFM mixes at 0, 1, 3, 7, and 28 days of SEM and EDX analysis were compared with XRD analysis. The intensity count of C-S-H compounds is higher than  $\text{Ca}(\text{OH})_2$  compounds, and no interruption of pozzolanic reactions is evident, which has a considerable favourable impact on the decrease of  $\text{Ca}(\text{OH})_2$ -(CH).

Furthermore, as per ACI 549.1R-93 and the WRD handbook, the mortars attained the required compressive strength. The results of splitting tensile and flexural strengths, and impact resistance show that the mixes used in this study can be used in ferrocement applications. Coconut husk can be used as an alternative sustainable material to produce both CCHM and CSCHSFM mixes. Without any doubt, this study found sustainable alternate materials for producing mortar from renewable resources and waste.

In the case of non-structural ferrocement elements, the strength being non-significant criteria, the CCHM mix can be adopted so that the self-weight of that element can be reduced. The CSCHSFM mix can be highly recommended for structural elements. This study concludes that using coconut husk as a fine aggregate in the manufacturing of mortar is viable, and the materials are undoubtedly sustainable alternative materials for making mortar, which is used for ferrocement techniques.

**Author Contributions:** K.K.: Investigation, resources, data curation, formal analysis, writing—original draft, visualization. G.K.: Conceptualization, methodology, supervision, writing—review and editing, validation. A.R.: Supervision, writing—review and editing, validation. All authors have read and agreed to the published version of the manuscript.

**Funding:** This research received no external funding.

**Institutional Review Board Statement:** Not applicable.

**Informed Consent Statement:** Not applicable.

**Data Availability Statement:** Not applicable.

**Acknowledgments:** The authors recognize the management at the SRM Institute of Science and Technology, for their role in this comprehensive research and the individuals who openly/incidentally supported this research. We acknowledge SRMIST for use of the high resolution scanning electron microscope (HR-SEM). We acknowledge the XRD facility at SRMIST for the set up with support from the MNRE, Government of India.

**Conflicts of Interest:** The authors declare no conflict of interest.

## References

1. Koehnken, L. *Impacts of Sand Mining on Ecosystem Structures, Process and Biodiversity in Rivers*; World Wide Fund for Nature (WWF): Gland, Switzerland, 2018; ISBN 978-2-940529-88-9.
2. *Sand and Sustainability: Finding New Solutions for Environmental Governance of Global Sand Resources*; United Nations Environment Programme: Nairobi, Kenya, 2019; ISBN 978-92-807-3751-6.

3. Rising Demand for Sand Calls for Resource Governance, Rising Demand for Sand Calls for Resource Governance WWF. 2019. Available online: <https://www.unep.org/news-and-stories/press-release/rising-demand-sand-calls-resource-governance> (accessed on 7 May 2019).
4. How the Demand for Sand Is Killing Rivers, How the Demand for Sand Is Killing Rivers. *BBC News*, 3 September 2017.
5. Mishra, A. Rajasthan SEES Spurt in Demand for Manufactured Sand in Past Year, Rajasthan Sees Spurt in Demand for Manufactured Sand in Past Year. 2018. Available online: <https://www.dnaindia.com> (accessed on 3 September 2018).
6. Chilamkurthy, K.; Marckson, A.V.; Chopperla, S.T.; Santhanam, M. A statistical overview of sand demand in Asia and Europe. In Proceedings of the International Conference UKIERE CTMC, Goa, India, 22–24 June 2016; Volume 16, pp. 1–15.
7. Moudgil, M. How Sand Mining Impacts Ecosystem. India Water Portal. 2018. Available online: <https://www.indiawaterportal.org/articles/how-sand-mining-impacts-ecosystem> (accessed on 24 July 2018).
8. Saviour, M.N. Environmental Impact of soil and sand mining: A review. *Int. J. Environ. Sci. Tech.* **2012**, *1*, 125–134.
9. Challenges to Construction Materials Excellence: Sand Supply and Demand, Construction Plus Asia. 2017. Available online: <https://www.constructionplusasia.com/hk/challenges-construction-materials-excellence-sand-supply-demand/> (accessed on 27 May 2017).
10. Florea, M.; Ning, Z.; Brouwers, H. Activation of liberated concrete fines and their application in mortars. *Constr. Build. Mater.* **2014**, *50*, 1–12. [[CrossRef](#)]
11. Ulsen, C.; Kahn, H.; Hawlitschek, G.; Masini, E.; Angulo, S.; John, V. Production of recycled sand from construction and demolition waste. *Constr. Build. Mater.* **2013**, *40*, 1168–1173. [[CrossRef](#)]
12. Singh, M.; Srivastava, A.; Bhunia, D. An investigation on effect of partial replacement of cement by waste marble slurry. *Constr. Build. Mater.* **2017**, *134*, 471–488. [[CrossRef](#)]
13. Naaman, A.E. Ferrocement and thin reinforced cement composites: Five decades of progress. *J. Ferrocem.* **2006**, *36*, 741.
14. Naaman, A.E. Ferrocement housing: Toward integrated high technology solutions. *J. Ferrocem.* **1989**, *19*, 141–149.
15. Naaman, A.E. Prospect in ferrocement materials, applications and technology. *J. Ferrocem.* **1985**, *15*, 165–167.
16. Building a Ferrocement Water Tank, Institute of Rural Development and Women’s Development Training Programme. The University of the South Pacific. 2022. Available online: <https://www.ircwash.org/resources/building-ferrocement-water-tank> (accessed on 12 June 2022).
17. Clarke, R.P.; Sharma, A.K. The Earthquake Strengthening of Single-Storey Unreinforced Block Masonry Houses in Trinidad and Tobago Using Ferrocement. International Ferrocement Society Representative for Trinidad and Tobago. Public Information Series/Earthquakes. 1977. Available online: <https://richardpclarke.tripod.com/hurri/manual.pdf> (accessed on 15 May 2022).
18. Shafiqh, P.; Mahmud, H.B.; Jumaat, M.Z.; Zargar, M. Agricultural wastes as aggregate in concrete mixtures—A review. *Constr. Build. Mater.* **2014**, *53*, 110–117. [[CrossRef](#)]
19. Prusty, J.K.; Patro, S.K.; Basarkar, S. Concrete using agro-waste as fine aggregate for sustainable built environment—A review. *Int. J. Sustain. Built Environ.* **2016**, *5*, 312–333. [[CrossRef](#)]
20. Pereira, C.; Savastano, H.; Payá, J.; Santos, S.; Borrachero, M.; Monzó, J.; Soriano, L. Use of highly reactive rice husk ash in the production of cement matrix reinforced with green coconut fiber. *Ind. Crop. Prod.* **2013**, *49*, 88–96. [[CrossRef](#)]
21. Memon, S.A.; Javed, U.; Khushnood, R.A. Eco-friendly utilization of corncob ash as partial replacement of sand in concrete. *Constr. Build. Mater.* **2018**, *195*, 165–177. [[CrossRef](#)]
22. Rafiezonooz, M.; Mirza, J.; Salim, M.R.; Hussin, M.W.; Khankhaje, E. Investigation of coal bottom ash and fly ash in concrete as replacement for sand and cement. *Constr. Build. Mater.* **2016**, *116*, 15–24. [[CrossRef](#)]
23. Wang, H.-Y.; Tsai, S.-L.; Hung, C.-C.; Jian, T.-Y. Research on engineering properties of cement mortar adding stainless steel reduction slag and pozzolanic materials. *Case Stud. Constr. Mater.* **2022**, *16*, 1–17. [[CrossRef](#)]
24. Pichór, W.; Kamiński, A.; Szoldra, P.; Fraç, M. Lightweight Cement Mortars with Granulated Foam Glass and Waste Perlite Addition. *Adv. Civ. Eng.* **2019**, *2019*, 1–9. [[CrossRef](#)]
25. Gameiro, F.; de Brito, J.; da Silva, D.C. Durability performance of structural concrete containing fine aggregates from waste generated by marble quarrying industry. *Eng. Struct.* **2013**, *59*, 654–662. [[CrossRef](#)]
26. Silva, J.; De Brito, J.; Veiga, R. Incorporation of fine ceramics in mortars. *Constr. Build. Mater.* **2009**, *23*, 556–564. [[CrossRef](#)]
27. Lam, M.N.-T.; Nguyen, D.-T.; Nguyen, D.-L. Potential use of clay brick waste powder and ceramic waste aggregate in mortar. *Constr. Build. Mater.* **2021**, *313*, 125516. [[CrossRef](#)]
28. Corinaldesi, V.; Moriconi, G.; Naik, T.R. Characterization of marble powder for its use in mortar and concrete. *Constr. Build. Mater.* **2010**, *24*, 113–117. [[CrossRef](#)]
29. Gunasekaran, K.; Annadurai, R.; Kumar, P.S. Study on reinforced lightweight coconut shell concrete beam behavior under flexure. *Mater. Des.* **2013**, *46*, 157–167. [[CrossRef](#)]
30. Gunasekaran, K.; Annadurai, R.; Kumar, P. Long term study on compressive and bond strength of coconut shell aggregate concrete. *Constr. Build. Mater.* **2012**, *28*, 208–215. [[CrossRef](#)]
31. Ramasubramani, R.; Gunasekaran, K. Sustainable Alternate Materials for Concrete Production from Renewable Source and Waste. *Sustainability* **2021**, *13*, 1204. [[CrossRef](#)]
32. Gunasekaran, K.; Kumar, P.S.; Lakshmiathy, M. Study on properties of coconut shell as an aggregate for concrete. *ICI J.* **2011**, *12*, 27–33.

33. Gunasekaran, K.; Kumar, P.; Lakshmipathy, M. Mechanical and bond properties of coconut shell concrete. *Constr. Build. Mater.* **2010**, *25*, 92–98. [[CrossRef](#)]
34. Gunasekaran, K.; Annadurai, R.; Kumar, P.S. A study on some durability properties of coconut shell aggregate concrete. *Mater. Struct.* **2013**, *48*, 1253–1264. [[CrossRef](#)]
35. *IS 12269*; Ordinary Portland Cement, 53 Grade—Specification. Bureau of Indian Standards: New Delhi, India, 2013.
36. *IS 383*; Coarse and Fine Aggregate for Concrete—Specification. Bureau of Indian Standards: New Delhi, India, 2016.
37. *ACI 549.1R-97*; Guide for the Design, Construction and Repair of Ferrocement. ACI Committee 549: Farmington Hills, MI, USA, 1997.
38. *ACI 549.1R-93*; State of the Art Report on Ferrocement. ACI Committee 549: Farmington Hills, MI, USA, 1999.
39. Ferrocement Technology. In *WRD Handbook*; Maharashtra Engineering Research Institute: Nashik, India, 2018.
40. Mehta, P.K.; Paulo, J.M.M. *Concrete, Microstructure, Properties and Materials*, 3rd ed.; Tata McGraw Hill Education Private Limited: New Delhi, India, 2006; Fourth reprint 2010.
41. Mollah, M.Y.A.; Hess, T.R.; Cocke, D.L. Surface and bulk studies of leached and unleached fly ash using XPS, SEM, EDS and FTIR techniques. *Cem. Concr. Res.* **1994**, *24*, 109–118. [[CrossRef](#)]
42. Stutzman, P. Direct determination of phases in portland cements by quantitative X-ray powder diffraction. *NIST Tech. Note* **2010**, *1692*, 59.
43. *IS 5512:1983*; Flow Table for Use in Tests of Hydraulic Cements and Pozzolanic Materials—Specification. Bureau of Indian Standards: New Delhi, India, 2004.
44. *ASTM C1437-20*; Standard Test Method for Flow of Hydraulic Cement Mortar. ASTM International Standards: West Conshohocken, PA, USA, 2021.
45. *ASTM C143/C143M-10*; Standard Test Method for Slump of Hydraulic-Cement Concrete. ASTM International Standards: West Conshohocken, PA, USA, 2007.
46. *ASTM C109/C109M-02*; Standard Test Method for Compressive Strength of Hydraulic Cement Mortars. ASTM International Standards: West Conshohocken, PA, USA, 2002.
47. *ASTM C496/C496-11*; Standard Test Method for Splitting Tensile Strength of Cylindrical Concrete Specimens. ASTM International Standards: West Conshohocken, PA, USA, 2004.
48. *ASTM C348-02*; Standard Test Method for Flexural Strength of Hydraulic-Cement Mortars. ASTM International Standards: West Conshohocken, PA, USA, 2002.
49. *ACI 544.2R-89*; Measurement of Properties of Fiber Reinforced Concrete. ACI Committee 544: Farmington Hills, MI, USA, 1999.
50. Mohit, M.; Sharifi, Y. Thermal and microstructure properties of cement mortar containing ceramic waste powder as alternative cementitious materials. *Constr. Build. Mater.* **2019**, *223*, 643–656. [[CrossRef](#)]
51. Prasad, D.D.; Kishore, R. Fourier transformed-infrared spectroscopy (FTIR) studies on the concrete/cement mortar mass made of cent percentage recycled coarse aggregate and fine aggregate. *Int. J. Adv. Res. Eng. Technol.* **2021**, *12*, 387–400. [[CrossRef](#)]
52. Muttashar, H.L.; Ali, N.B.; Ariffin, M.A.M.; Hussin, M.W. Microstructures and physical properties of waste garnets as a promising construction materials. *Case Stud. Constr. Mater.* **2018**, *8*, 87–96. [[CrossRef](#)]
53. Brekailo, F.; Pereira, E.; Pereira, E.; Farias, M.M.; Medeiros-Junior, R.A. Red ceramic and concrete waste as replacement of portland cement: Microstructure aspect of eco-mortar in external-sulfate attack. *Clean. Mater.* **2021**, *3*, 100034. [[CrossRef](#)]
54. Singh, M.; Siddique, R. Strength properties and micro-structural properties of concrete containing coal bottom ash as partial replacement of fine aggregate. *Constr. Build. Mater.* **2014**, *50*, 246–256. [[CrossRef](#)]
55. Ortega, J.M.; Letelier, V.; Solas, C.; Moriconi, G.; Climent, M.; Sánchez, I. Long-term effects of waste brick powder addition in the microstructure and service properties of mortars. *Constr. Build. Mater.* **2018**, *182*, 691–702. [[CrossRef](#)]
56. Stutzman, P.E.; Bullard, J.W.; Feng, P. Phase Analysis of Portland Cement by Combined Quantitative X-ray Powder Diffraction and Scanning Electron Microscopy. *J. Res. Natl. Inst. Stand. Technol.* **2016**, *121*, 47–107. [[CrossRef](#)] [[PubMed](#)]
57. *IS 4031(Part 7)-1988*; Methods of Physical Test for Hydraulic Cement. Bureau of Indian Standards: New Delhi, India, 2005.
58. Liao, Y.; Wang, X.; Wang, L.; Yin, Z.; Da, B.; Chen, D. Effect of waste oyster shell powder content on properties of cement-metakaolin mortar. *Case Stud. Constr. Mater.* **2022**, *16*, 1–13. [[CrossRef](#)]
59. Bouvet, A.; Ghorbel, E.; Bennacer, R. The mini-conical slump flow test: Analysis and numerical study. *Cem. Concr. Res.* **2010**, *40*, 1517–1523. [[CrossRef](#)]
60. Zhou, B.; Zhang, M.; Wang, L.; Ma, G. Experimental study on mechanical property and microstructure of cement mortar reinforced with elaborately recycled GFRP fiber. *Cem. Concr. Compos.* **2020**, *117*, 103908. [[CrossRef](#)]
61. Ede, A.N.; Agbede, J.O. Use of coconut husk fiber for improved compressive and flexural strength of concrete. *Int. J. Sci. Eng. Res.* **2015**, *6*, 968–974.

**Disclaimer/Publisher’s Note:** The statements, opinions and data contained in all publications are solely those of the individual author(s) and contributor(s) and not of MDPI and/or the editor(s). MDPI and/or the editor(s) disclaim responsibility for any injury to people or property resulting from any ideas, methods, instructions or products referred to in the content.